Review

Green Catalysts: Applied and Synthetic Photosynthesis

This contribution is dedicated to Professors Ana and Tom Moore : Mentors, Colleagues, Friends, and Early Visionaries

Alexandra H. Teodor [1], Benjamin D. Sherman [2], Zeah Yvette Ison[3], Eu-Jee Ooi[4], Jesse J. Bergkamp[5], Barry D. Bruce [1,6,7]*

[1] Graduate School of Genome Science and Technology, University of Tennessee at Knoxville and Oak Ridge National Laboratory; ateodor@vols.utk.edu
[2] Department of Chemistry and Biochemistry, Texas Christian University; B.D.SHERMAN@tcu.edu
[3] Department of Chemistry and Biochemistry, California State University Bakersfield; zison@csub.edu
[4] Department of Chemistry and Biochemistry, California State University Bakersfield; eooi@csub.edu
[5] Department of Chemistry and Biochemistry, California State University Bakersfield; jbergkamp@csub.edu
[6] Department of Chemical and Biomolecular Engineering, University of Tennessee at Knoxville
[7] Biochemistry, Cellular & Molecular Biology Department, University of Tennessee at Knoxville

* Correspondence: bbruce@utk.edu; Tel.: +1-865-974-4082

Abstract: The biological process of photosynthesis was critical in catalyzing the oxygenation of Earth's atmosphere 2.5 billion years ago, changing the course of development of life on Earth. Recently, the fields of applied and synthetic photosynthesis have utilized the light-driven protein-pigment supercomplexes central to photosynthesis for the photocatalytic production of fuel and other various valuable products. The reaction center Photosystem I is of particular interest in applied photosynthesis due to its high stability post-purification, non-geopolitical limitation, and its ability to generate the greatest reducing power found in Nature. These remarkable properties have been harnessed for the photocatalytic production of a number of valuable products in the applied photosynthesis research field. These primarily include photocurrents and molecular hydrogen as fuels. The use of artificial reaction centers to generate substrates and reducing equivalents to drive non-photoactive enzymes for valuable product generation has been a long-standing area of interest of the synthetic photosynthesis research field. In this review, we cover advances in these areas and further speculate synthetic and applied photosynthesis as photocatalysts for the generation of valuable products.

Keywords: Photosynthesis; Photoelectrochemical Devices; Biohybrid; Synthetic Biology; Photochemistry; Photoelectrochemistry; Hydrogen Evolution

1. Introduction

The generation of electricity through renewable, sustainable means is a crucial step for meeting future anthropocentric energy demands. Several renewable energy technologies have been utilized, such as wind, geothermal, hydroelectric, and wave/tide generators. However, these technologies are dependent on local resources and are therefore location-limited. One energy resource that is of great interest and abundantly widespread is solar energy that can be captured through photovoltaics technology. Converting solar energy via applied and synthetic photosynthesis could lower society's dependence on fossil fuels. Applied Photosynthesis takes inspiration from and utilizes the fundamental mechanisms and components that Nature has already developed for biological photosynthesis, specifically the light reactions of biological photosynthesis.

Incorporating biological light-absorbing pigments into otherwise man-made devices is an attractive approach for converting solar energy into electric potential or fuels due to their high internal quantum efficiency of charge separation, nontoxic nature, and carbon-neutral production. One such device is the dye-sensitized solar cell (DSSC). DSSCs have recently gained the attention of many researchers. The fundamental charge generation processes in DSSCs are similar to those found in natural photosynthesis, and are as follows: a chromophore absorbs a photon, producing the dye excited state. The excited state transfers an electron to an n-type semiconductor support which results in current flow from the photoanode to cathode in the cell. The resulting surface oxidized dye regenerates the ground state by electron transfer from a reduced redox mediator in solution, and the oxidized form of the mediator is then re-reduced at the cathode to complete the electric circuit of the cell. This process allows the stable conversion of photon energy to electric potential energy which could also be used to drive net catalytic redox reactions to give a photoelectrosynthetic cell in place of a photovoltaic device, such as a DSSC.

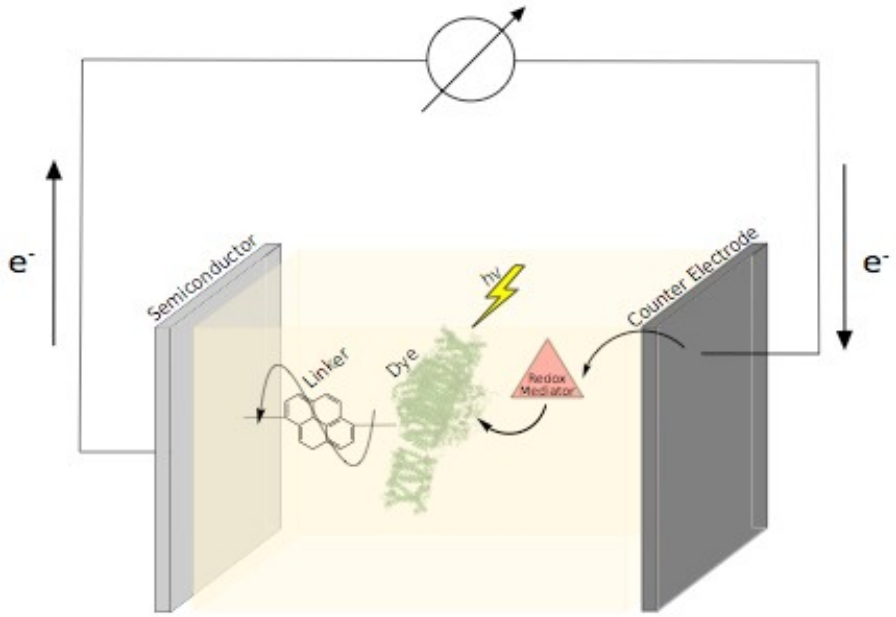

Figure 1. General schematic showing the key working components of a bio-hybrid solar cell. The figure shows a bio-absorber (dye), after light excitation donating an electron through a linker to a semiconductor surface. This electron is then passed to the counter electrode where it interacts with a redox mediator that reduces the oxidized bio-absorber and completes the circuit.

Similarly, the first stage of photosynthesis requires a photon to be absorbed by pigments bound within protein complexes in a light-harvesting antenna, promotion of an electron to an excited state and then subsequent charge-separation followed by multiple electron-transfer steps. Reaction centers such as Photosystem I (PSI), Photosystem II (PSII), and bacterial reaction centers from organisms such

as the purple bacterium *Rhodobacter sphaeroides* (*R. sphaeroides*) are examples of such protein-pigment supercomplexes, and they operate at internal quantum efficiencies approaching 100%. PSII performs the biological oxidation of water at +1.2 V vs SHE utilizing a Mn_4O_5Ca oxygen evolving complex to generate electrons. In turn, PSI generates the greatest reducing potential found in Nature of -1.2 V vs SHE, yielding highly reducing electrons which go on to power ATP and NADH generation along with carbon fixation *in vivo* in photosynthetic organisms. Reaction centers perform their primary charge separation activity via a special pair of pigments. In PSI this charge separation occurs with an exceptionally high quantum efficiency of near 100%, far above that of many synthetic photosensitizers utilized in inorganic DSSCs, and an electron transfer rate reported to approach 50 $e^- s^{-1}$ PSI^{-1} *in vivo*[1]. Further, PSI and other biological photosensitizers are relatively low cost and carbon neutral to produce, with easy waste management as compared to other photosensitizers, making them of interest for the generation of carbon-neutral, sustainable devices [2].

Another area of interest for the generation of fuels and other valuable products takes inspiration from the biological photocatalytic process of photosynthesis, that of synthetic photosynthesis. Instead of utilizing biological materials such as pigments or reaction centers for performing the initial conversion of photonic to electronic energy that are then incorporated into inorganic devices, synthetic man-made reaction centers perform the initial conversion of photonic energy which are then coupled to drive non-photoactive biological enzymes for product generation. Since this bio-hybrid uses non-toxic and highly selective enzymes and takes advantage of their high catalytic turnover rates, this area is of increasing interest for the sustainable generation of valuable chemical products. This approach is similar to photosynthetic organisms, who do not directly couple their photochemical reactions to terminal catalysis, instead performing the chemical reactions in a controlled, step-wise manner through a limited subset of reactive chemical species that power the enzymatic catalysis of substrates.

In this review, we cover recent advances and areas of focus in these two research areas of applied and synthetic photosynthesis, specifically on photocurrent and molecular hydrogen production through applied photosynthesis, and generation of valuable products through artificial photosynthesis. We also speculate on areas of improvement and future directions for these bio-inspired photocatalysis research fields.

2. Applied Photocurrent

This section reports the most recent advances of photocurrent generation by photosynthetic protein-pigment complexes incorporated into devices for energy or valuable product generation. We focus on the reaction centers PSI and PSII and the light-harvesting antennas Light Harvesting Complex I (LHC I) and Light Harvesting Complex II (LHC II) being used as the primary photocatalysts for these applications. Many advances discussed herein include the studies of electrode materials and semiconducting surfaces, redox mediators, chemical modification, and some examples of photoprotection for device stability.

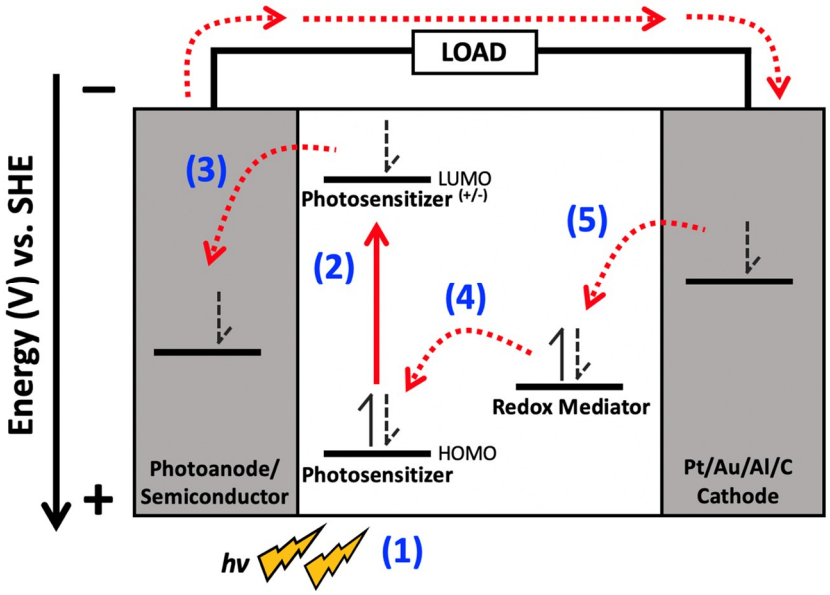

Figure 1. Representation of electron transfer in a photovoltaic device. This is comprised of a photosensitive dye(s), semiconductors, and electrolyte (redox mediator). In order for forward electron injection from a dye to a semiconductor to take place the LUMO must have a more negative potential than the semiconductor. The electrolyte must bear a more negative potential then dye^{+}. The steps of electron transfer are as follows: (1) first, the photosensitizer (PSI) absorbs a photon, and (2) the photosensitizer is then promoted to an excited state. Next, charge separation by the photoexcited sensitizer occurs, and (3) the excited electron is injected into the conduction band of the semiconductor. (4) The photosensitizer is then reduced by the redox mediator in the electrolyte, priming it for further photoexcitation events to generate more photocurrent. Finally, (5) the redox mediator is reduced in turn at the counter-electrode, completing the circuit. Adapted from [3].

2.1. *Light absorption, electronic considerations, and optical cross-sections of reaction centers*

Researchers have shown that optimal energetics of electron transport pathways occur when photoactivated biohybrid energy harvesting constructs involve PSI interacting with a soluble carrier, a solid-state electrode, or bound catalysts [4]. PSI, PSII, and LHC I & II are biological supercomplexes composed of both proteinaceous subunits along with pigments and other redox-active cofactors. These protein-pigment complexes function as light absorbers and energy converters that are active over large specific regions of the UV-Visible spectrum based on the primary pigments present in their light harvesting antennas. There is a general consensus in the applied photosynthesis field that PSI can further be modified for optimal energy conversion by modification of absorption wavelengths, which is a property of the biohybrid material, and through the incorporation of selective biocompatible electrodes, mediators, and composite matrices in systems for solar energy conversion, or photocatalysis [5]. Enhancement of the optical cross-section of photosensitizers to extend their photoexcitation capabilities is one strategy of interest for increasing the output of these photocatalysts. In this section, we will focus on the progress made in the studies that include information on, or involve, light absorption and electronic considerations of reaction centers. In Figure 3 below, we show the optical cross sections of the biological reaction centers and synthetic dyes discussed in this section.

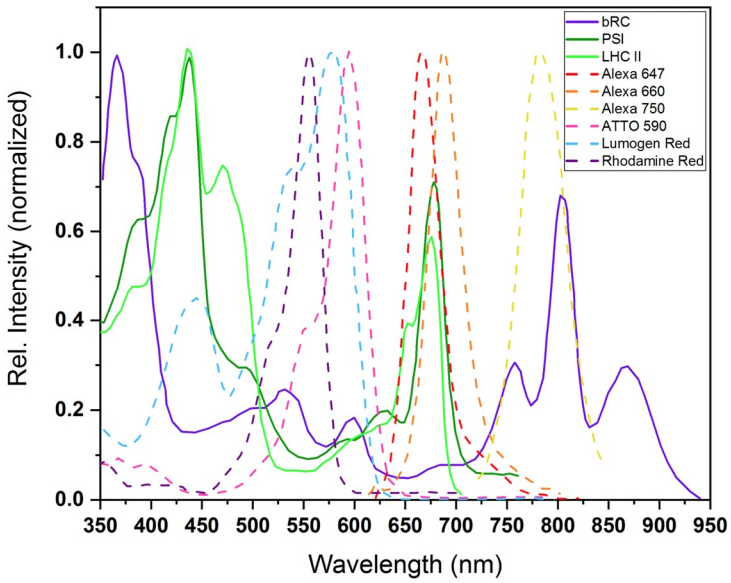

Figure 3. Optical cross-sections of reaction centers and dyes. The UV-Visible absorption spectra of commonly studied biological reaction centers and dyes used to extend their optical cross-sections are shown. The maxima of each spectra were normalized to 1.0 for comparison.

One research group studied the photoelectrochemistry of PSI immobilized on a photoelectrode surface and found that upon illumination with a 676 nm band-pass filtered light at 1.4 mW cm^{-2}, a photocurrent of 4 μA cm^{-2} is obtained [6]. This 676 nm light is near the optimal excitation wavelength for PSI. However, the efficiency of PSI electron generation through the absorption of incident photons is limited by its poor absorption in the "green gap" of its absorption spectrum[7]. One approach to increase the optical cross-section of reaction centers is the incorporation of synthetic dyes that absorb in different regions of the UV-Vis spectrum, enabling a transfer of energy from the dyes to the reaction center [7]. Dye-modified PSI activity has been shown to be enhanced even in solid state devices as evident via surface photovoltage (SPV) experiments [7].

Dyes have also been conjugated to photosynthetic reaction centers and light-harvesting antennas beyond PSI in attempts to enhance their optical cross-sections, and thus, their ability to be photoactivated. The use of dyes to fill in the "green gap" of chlorophyll-based protein-pigment complexes has been studied for the last decade. One of the earlier reports on modulating optical cross-sections assessed synthetic porphyrin and chlorin dyes with a variety of side groups and their spectral properties and ability to self-assemble into biomimetic light-harvesting antenna systems [8]. The highly ordered nature of these dyes, similar to the order of pigments in biological protein-pigment complexes, allowed for photoexcitation even when aggregated and the photochemical efficiency was unaffected [9]. The ability to couple together different dyes in synthetic biomimetic systems to enhance light harvesting capabilities led to interest in the conjugation of dyes to biological reaction centers like PSI to similarly supplement their optical cross-section.

One report on dyes conjugated with a biological protein-pigment complex used recombinant LHC II, a PSI- and PSII- light harvesting antenna complex and either one or three Rhodamine Red dyes covalently attached via cysteine residues on the protein [10]. Dye addition did not affect the assembly, stability or activity of LHC II. While labelling efficiencies were low, electron transfer efficiency to LHC II was near 100%. Other dyes that have been similarly utilized include Alexa Fluor 660, 647, and 750 dyes, yielding similarly improved photogeneration of charge separated species while maintaining protein stability [11]. To date, the dyes Lumogen Red and ATTO 590 have been utilized to fill in the "green gap" of PSI. The coupling of approximately 30 ATTO 590 dye molecules to PSI increased the oxygen consumption activity of PSI by over 4-fold, and the addition of Lumogen Red allowed for greater energy transfer to PSI via Förster resonance energy transfer. Expanding the

light harvesting capabilities of PSI through conjugation of dyes [7, 12] is likely to be an area of further focus for improving outputs of future reaction center-based biohybrid devices.

Artificial metal nanoparticle antennas can also be used to enhance PSI light absorption and PSI circular dichroism over the protein's entire absorption band as opposed to the utilization of spherical metal nanoparticles (NP), which enhances only specific plasmon resonance wavelengths [13]. Metal NP aggregates, due to the high dielectric constant of the metal, and NP-PSI-NP antenna junctions cause broad-resonant and nonresonant electronic field enhancements, as well as enhancing PSI's light absorption capabilities [13]. Some researchers were able to achieve a 100% quantum efficiency with an integrated photoexcited PSI in solar energy conversion devices as the photoactive electrode [14]. Ag NPs have been found to enhance chlorophyll fluorescence up to 18-fold in peridinin-chlorophyll-protein assemblies, and 5- to 20-fold for thin films of cyanobacterial PSI [15, 16]. Similarly, incorporation of Au NPs in leaves and chloroplasts in vivo increased reaction center reduction rates [17]. While metal NPs may not directly expand optical cross-sections, enhancement of the photoelectrochemical activity of reaction centers, including PSI, should lead to improved photocurrent outputs of devices. The use of metal nanostructures, such as nanopyramids[18] and NPs have been suggested to enhance photochemical activity through plasmonic coupling, and further engineering to enhance interactions of this biotic-abiotic interface is likely to be studied for further biohybrid device improvement [19].

Quantum dots (QDs) have also been incorporated with photosynthetic reaction centers in attempts to enhance their photoelectrochemical properties and activities. The optoelectronic properties of QDs are as a function of both size and shape[20], allowing for fine-tuning to enhance their optical cross section. QDs have previously been shown to be capable of transferring their photoexcitation energy to reaction centers, including PSI[21, 22]. Reaction center charge separation has been found to increase anywhere from 3-5 fold upon QD conjugation. A study assessing the interaction of CdTe QDs with the Rhodobacter sphaeroides reaction center found that use of a polyhistidine tag on the reaction center allowed for targeted binding of the QD to the tag, and up to ~95% QD labeling efficiency was achieved as well[23]. The ability to now fine-tune the optoelectronic as well as binding properties of QDs makes this an area with great potential for further enhancement of biological photosynthetic reaction centers as light-activated catalysts.

2.2. *Novel semiconductor materials, architectures, and electrode surface modifications*

There are several publications on inorganic materials and surface shape used as semiconductors for biohybrid devices in the applied photosynthesis field. By improving the interface between the biological and inorganic portions of biohybrid devices, the aim is to increase the compatibility and further improve both outputs and rates of constructive forward electron transfer in devices. In this section, we will highlight recent advances in multiple methods for enhancing photosensitizer attachment and activity with semiconductors, including covalently linking reaction centers, intermolecular forces, and electrostatics along with novel semiconductor materials and architectures.

2.2.1. Semiconductor materials, architectures, and modifications

Novel semiconductor materials for biohybrid-based devices are of interest in the applied photosynthesis community to promote stronger affinity of the photosensitizer (PSI, PSII, bacterial reaction center) with the working electrode and enhance the biocompatability. Further, the electronic properties of the semiconductor material itself must be considered so that both charge collection and forward electron transfer from the photosensitizer reaction center occur at a rate that outcompetes the back-reaction and charge recombination of the photosensitizer. Further, the conduction band of the semiconductor must be well matched for forward electron injection from the biological photosensitizer with minimal wasted energy, and electron injection into the working electrode material. The use of semiconductor materials with these properties, along with the necessary

biocompatibility, has led to many research studies on this particular method of improving biohybrid device output.

One of the most commonly used and well-studied semiconductors for DSSCs in general, as well as specifically for biohybrid devices, is titanium dioxide (TiO_2). Isolated and purified biological pigments along with PSI and spinach LHCII can be spontaneously adsorbed in an active manner on three types of TiO_2 films [24]. The ability to engineer TiO_2 into novel semiconductor nanostructures has been well studied, as the ability to form 3D semiconductor architectures can dramatically increase the surface area of the electrode, permitting several orders of magnitude improvement in the amount of photosensitizer active in the biohybrid device. In addition to increased photosensitizer loading, increased contact with redox electrolytes is also achieved with 3D nanostructured semiconductor materials [25]. Some 3D structures utilized to date include TiO_2 nanoparticles (NPs), nanotubes, nano-pyramids, and inverse opal designs [26, 27] [18, 28].

There have been reports on the use of metal-binding peptides fused onto both reaction centers and redox mediator proteins to help increase coverage on semiconductor surfaces. Subunits of PSI have been recombinantly produced with ZnO binding peptides (ZOBiP-PSI), and TiO_2 binding peptides (TOBiP) have been fused to ferredoxin, the native biological acceptor of electrons from PSI to yield TOBiP-Fd. PSI can be chemically cross-linked with TOBiP-Fd on its acceptor side, and these PSI-Fd-TOBiP fusions along with ZOBiP- and MOBiP-PSI complexes show greater affinity upon incubation with various metal oxide nanoparticles for the semiconductor materials as compared to the native protein [29]. Use of the native electron acceptor partner, ferredoxin, may also help to increase forward electron transfer rates and reduce changes of PSI charge recombination occurring.

Some novel semiconductor materials being studied include gallium arsenide, carbon nanotubes or nanoparticles, and other nanorods or nanoparticles made from TiO_2, silicon, graphene, and gold. Further modification of the semiconductor surface by using conductive films composed of Nafion or Os polymers, oxides, metal nanoparticles, p-doped silicon, alkanethiolate self-assembled monolayer/Au, and graphene influence the production of photocurrent.

One such study utilized hematite as a semiconductor material with PSI. A biophotoanode performed electronic coupling between a red algal PSI associated with its light harvesting antenna LHCI and nanocrystalline n-typed semiconductors, such as TiO_2 and hematite (α-Fe_2O_3), through a structured multilayer of PSI-LHCI over both semiconductors organized as highly ordered nanocrystalline arrays [30]. The α-Fe_2O_3/PSI-LHCI organization is prepared by immobilizing the PSI-LHCI complex with its reducing side towards the α-Fe_2O_3 surface and nano structuring the multilayer in such a way to organize the subsequent complex layers in a head-to-tail orientation [30]. This biophotoanode operated at the highest quantum efficiency and generated the largest open circuit photocurrent reported to date as compared to the tandem system based on TiO_2/PSI-LHCI material[30].

The integration of large membrane proteins like reaction centers into rapidly prepared composite films needs to be a controlled process. One way this can be performed is through the use of potentiostatic electropolymerization from an aqueous solution containing both polymer and PSI to prepare polymer-protein films on Au electrodes [31].A novel preparation with poly(3,4-ethylenedioxythiophene)/single walled carbon nanotube (PEDOT/SWCNT) composite films with 0-50 wt.% SWCNT contents utilized a vapor phase polymerization technique [32]. A 35 wt.% SWCNT provides a maximum power factor of 37.8 $\mu W\ mK^{-2}$, which is 1.7 times higher than polymer-protein films prepared without SWCNTs [32].

The use of carbon-based semiconductor materials such as SWCNTs has been an area of increasing interest in the applied photosynthesis field. A high photocurrent generation and efficiency of a graphene-biohybrid light-harvesting electrode has been observed when it consisted of cyanobacterial trimeric PSI complexes immobilized onto π-system-modified graphene electrodes[33]. Cyanobacterial PSI on glassy carbon electrodes (GCE) modified with multi-walled carbon nanotubes (MWCNTs) using carboxylated pyrene derivative achieved covalent fixation of PSI [34]. There is a strong interaction between conjugated aromatic compounds, such as graphene, due to π–π-stacking

capabilities to adsorb PSI onto a graphene-modified surface via electrostatic interactions [33]. A pyrene-based graphene-PSI biohybrid system produced high photocurrent outputs up to 23-135 μA cm^{-2} [33].

Different polycyclic aromatic compounds can act as an interface between PSI and graphene-based semiconductors while supporting the electrochemical communication of the biomolecule with the electrode [35]. A PSI/polyaniline composite film best performed when deposited to a film thickness of 185 nm, yielding an over 200-fold improvement in photocurrent output over a traditionally deposited PSI multilayer film of similar thickness [31]. pH-dependent poly(vinyl)imidazole osmium bis(2,2′-bipyridine)chloride redox polymer has also been utilized to improve electronic contact with PSI, yielding an electron transfer rate of up to 335±14 e^{-} s^{-1} $PS1^{-1}$ [1]. A completely organic, optically transparent electrode can be constructed by using reduced graphene oxide (RGO) on which a functional plant PSI multilayer can be deposited [36].

In 2012, the integration of PSI films with p-doped silicon resulted in the highest reported photocurrent enhancement for a PSI biohybrid electrode [37]. Performing confined-plume-chemical deposition (CPCD) enabled the construction of a semiconductor-biological interface for solar energy conversion that optimizes biological and other temperature-sensitive substrates [38]. Depositing a crystalline material zinc oxide (ZnO) anode on PSI/p-doped silicon films via CPCD helped prevent damage to the PSI biomaterial and the need for seeding crystals [38]. Another way to maintain stable, electrochemically active PSI is to encapsulate it in a conductive polymer, such as Nafion, which acts as a support matrix for PSI electrodes [6]. Optimal effectiveness and efficiency are found in biohybrid solar cells that consisted of PSI/Nafion films, specific mediators and polymers, a 10 μg cm^{-2} surface density, and a 100 μg cm^{-2} photoactive protein loading surface density [6].

2.2.2. Electrode materials and modifications

The modification of a surface to improve biocompability and constructive interactions at the biological-inorganic interface is necessary to establish good contact between the material and reaction center, which allows for electron transfer or interaction. The surface interactions and adsorption of PSI onto electrodes or semiconductors could include self-assembled monolayers (SAMs), as well as molecular tethers or peptide segments containing carboxylic acid anchoring groups, alcohols, and thiols.

A novel biomimetic approach for an effective assembly of PSI with the electron transfer carrier cytochrome c_6 (cyt c) deposited on a thiol modified gold surface was reported in 2014 [39]. Cyt c_6 acts as the *in vivo* reducer of PSI in cyanobacterial photosynthesis. This approach involved using cyt c as a template for the assembly of an oriented, densely packed PSI layer as well as a wiring agent to direct electrons from the electrode towards PSI [39]. An intermittent cyt c layer was necessary in this study for an efficient connection of PSI layers with the electrode, as well as for enhanced photocurrent density [39]. Further work on cytochromes yielded five distinct bioengineered hexahistidine (His6)-tagged cytochrome c_{553} (cyt c_{553}) variants by introducing the specific linker peptides of 0–19 amino acids (AA) in length between the cyt c_{553} holoprotein and a C-terminal His6-tag affinity tag used for specific immobilization on the semiconductor surface [40]. This yielded a significantly higher number of feasible conformations of immobilized cyt c variants when longer, more flexible linker peptides were utilized. Tagged cyt c_{533} was able to biopassivate the semiconductor substrate, giving these biohybrid photoelectrochemical cells some characteristics of the p-n-type diodes, although varying dark saturation current level ($J0$) considered as the charge recombination parameter [40].

PSI has been immobilized on nanoporous gold leaf (NPGL) electrode surfaces to give a light intensity-dependent photoinduced electric current [41]. Gold is a commonly utilized electrode material in biohybrid electrodes and devices due to its high conductivity and biologically inert nature. Au can be functionalized for covalent protein binding with 3-mercapto-1-propane-sulfonate and 2,2′-dimethyl-4,4′-bipyridine to form a self-assembled monolayer (SAM) [42]. A uniform PSI monolayer assembled on C9 alkanethiolate SAM/Au surfaces has increased photocurrent density with

increasing dissolved oxygen concentrations, potentially from oxygen helping to drive forward electron transfer from PSI by acting as an electron acceptor [4]. The PSI-mediated electron transfer for an analogous 2D system can be improved through dealloying, which would sufficiently enlarge the pores on the electrode surface [41]. Another cross-linker, 2-iminothiolane (2IT), is capable of connecting protein molecules with covalent bonds to metal surfaces. 2IT was used to stabilize PSI multilayer films on gold substrates against significant desorption and degradation upon addition of the liquid electrolyte solution and upon performing photoelectrochemical activity, with superior thickness retainment of the cross-linked PSI films compared to non-crosslinked films [43].

A biohybrid photoanode of PSII extracted from fresh spinach entrapped on mesoporous tungsten oxide (WO_3) film can be fabricated on fluorine-doped tin oxide. This architecture communicates with the WO_3 electrode in the absence of any soluble redox mediators and sacrificial reagents under the visible light of the solar spectrum up to 700 nm [44].

2.3. *Redox mediators*

Beyond electrode materials and architectures, the performance of biohybrid devices can be improved with redox mediators, which assist in both directing electrons to the biological photosensitizer and in enhancing conductivity between the electrodes. Upon photo-oxidation, it is necessary for the photosensitizer (such as PSI) to be reduced for another photo-oxidation event to occur. Mediators with suitable redox potentials for accepting electrons are an essential component to the conversion of light to energy. However, not all redox mediators are suitable for biohybrid photoelectrochemical devices. The traditional DSSC I^-/I_3^- redox mediator is corrosive to both protein and metal, has a midpoint potential similar to PSI, and intensely absorbs light in the visible spectrum [45]. Generation of reactive oxygen species in devices operated under aerobic operation compromises the long-term stability of photosynthetic biophotoelectrodes, even though molecular oxygen can help reduce PSI charge recombination rates ([46]. Under anaerobic conditions, the operation of a PSI-based photocathode using an electron acceptor that enables photocurrent generation can substantially improve stability and allow for exposure to higher light intensities [46].

Further, the transfer of electrons to and from reaction centers is much slower than the primary charge separation events of these photosensitizers, and the ability and rate of electron donation/acception of mediators with photosensitizers plays a key role in biohybrid device performance at the solution-electrode interface as governed by Butler-Volmer kinetics [47]. Publications on research involving redox mediators include small organic-based molecules, such as methyl viologen (MV), 2,6-Dichlorophenolindophenol (DCPIP), and ferricyanide complexes. Organometallic redox mediators include cobalt-, ruthenium-, and osmium-based complexes typically coordinated by bipyridine ligands. Solid-state electrons can be shuttled and be donated to a secondary acceptor via organic polycationic polymers, such as polyviologens [14]. There are multiple studies utilizing the biological PSI electron donor cyt c_6 as well. However, this is one of the least-studied areas of biohybrid photoelectrochemical electrodes and devices, and is likely an area where significant improvements in performance could be made.

One commonly used class of molecules as diffusible sacrificial electron mediators in PSI-based systems are MV [14]. MV can also be used as a charge carrier for the collection of electrons at the reduced F_B PSI site, as it can act as an acceptor of electrons from PSI [48]. Photoexcited PSI has also been shown to interact with polyviologens in solid state devices. PSI/polyviologen protein surfaces immobilized in Nafion polymer have been shown to significantly enhance photocurrent, aid in electron transfer, stabilize PSI through immobilization, and enhancing electrolyte conductivity [14]. Lower Nafion concentrations have been shown to increase redox mediator diffusivity with both $Os(bpy)_2Cl_2$ and MV redox mediators [6]. As another alternative redox mediator, cobalt complexes can be used in PSI biohybrid solar cells because they are not corrosive and they offer more negative redox potentials to drive the reduction of PSI [45].

Preprints (www.preprints.org) | NOT PEER-REVIEWED | Posted: 10 August 2020 doi:10.20944/preprints202008.0234.v1

Peer-reviewed version available at Catalysts 2020, 10, 1016; doi:10.3390/catal10091016

PSI integrated within a redox hydrogel polymer acts as a conducting matrix for the transfer of electrons from electrode surfaces to the photooxidized PSI [48]. Oxygen drives MV to initiate a light-induced unidirectional electron transfer, which results in photocurrent from an electron donor Au surface via surface assembled PSI trimers. PSI wet cells typically use MV and either ferrocyanide mediators or osmium-base mediators. In PSI/SAM/Au systems, dissolved oxygen in solution forms a complex intermediate species with MV to mediate redox pathways[4].

Developments with devices involving PSI-based light conversion to electrical energy have increased the knowledge of materials and methods that optimize the photocurrents and photovoltages generated [49]. We have systematically analyzed research articles concerning PSI-based biohybrid devices published within the past decade. Table 1 and Table 2 briefly summarize some of the key characteristics of plant and cyanobacterial PSI-based biohybrid solar cells that include a value for photocurrent and have been recently investigated.

Table 1. Photocurrent Analysis of Higher Plant PSI-based Biohybrid Devices[†]

Electrode Surface/Immobilization	Redox Mediators	Photocurrent (μA cm^{-2})	Current Density (μA cm^{-2} mW^{-1})	Ref.
Terephthalic -dialdehyde-SAM on nanoporous gold	Sodium ascorbate; 2,6-dichloroindophenol	0.3	0.08	[41]
Bare gold	Sodium ascorbate; 2,6-dichlorophenolindophenol	N/A	0.1	[50]
PSI-based biohybrid cells	Sodium ascorbate; 2,6-dichloroindophenol	2	0.138	[51]
PSI films/p-doped silicon	Methyl viologen	875	4.6	[37]
PSI multilayer/ reduced graphene oxide	Ferrocyanide; Methylene blue; Sodium ascorbate; Methyl viologen; 2,6-dichlorophenolindophenol; Ruthenium(II) hexamine	1.2	N/A	[36]
PSI multilayer film on gold	Ferricyanide	0.9	N/A	[5]
Polyaniline-PSI film on gold surface	Sodium ascorbate	5.7	N/A	[31]
PSI-polyaniline/Titanium dioxide	Methyl viologen	72	N/A	[52]
Solid-state unetched p-doped silicon/PSI	Methyl viologen	Non-etched: 21 Etched: 127	N/A	[38]
PSI multilayer film/SAM on gold-coated silicon	Osmium-based redox hydrogel	2-iminothiolane-crosslinked: ~8	N/A	[43] [b]
PSI/poly(3,4-ethylene-dioxythiophene):poly-styrenesulfonate/fluorine-doped tin oxide	N/A	960	N/A	[2]
PSI multilayer film/gold/SAM/aminoethanethiol	$[Fe(CN)6]^{4-}$; $[Fe(CN)6]^{3-}$	0-0.84 for PSI film thickness 0-1.3 um	N/A	[47]
PSI/p-doped silicon	Methyl viologen; Polyviologen	N/A	N/A	[14]

[†] PSI-based biohybrid solar cells component information with its respective generated photocurrent. PSI source is the spinach plant. Electron donors and acceptors are indicated under the redox mediators' category. The photocurrents are reported in μA cm^{-2}. Any unavailable, multiple, or estimated data is indicated with (N/A).

[a] Reference was conducted to improve the photocurrent performance of PSI-based biohybrid cells.

[b] Reference did not report current density.

[c] Reference reported other estimated photocurrent values observed in different conditions or solar cell composition.

Table 2. Photocurrent Analysis of Cyanobacterial PSI-based Biohybrid Devices‡

PSI Source	Electrode Surface/ Immobilization	Redox Mediators	Photocurrent ($\mu A\ cm^{-2}$)	Current Density ($\mu A\ cm^{-2}\ mW^{-1}$)	Ref.
T. elongatus	PSI/SAM on gold surface	Sodium ascorbate	0.088	N/A	[42][a]
T. elongatus	PSI/Nafion film	Osmium bis(2,2′-bipyridine)chloride; Methyl viologen	4	N/A	[6]
T. elongatus	PSI/osmium-complex-modified polymer	Methyl viologen; Osmium-based redox hydrogel	N/A	322	[1] [a]
T. elongatus	PSI/thiol-modified gold	Ascorbate-reduced 2,6-dichloroindophenol; Methyl viologen	1	0.97	[39][a]
T. elongatus	PSI/pi-system-modified graphene	Methyl viologen	135	N/A	[33][b]
HT3 cells	PSI/1D nanostructured titanium dioxide thin films	Sodium ascorbate; 2,6-dichlorophenolindophenol	4150	N/A	[53]
T. elongatus	ZOBiP-PSI- or TOBiP-Fd-PSI-based biohybrid dye-sensitized solar cells	Cyt c_6	N/A	N/A	[29][a]
T. elongatus	PSI/Transparent mesoporous indium tin oxide	N/A	150	N/A	[54]
T. elongatus	PSI on C_9 alkanethiolate SAM/Au	Methyl viologen	0.006	N/A	[4]
T. elongatus	PSI/pi-system-modified graphene	Methyl viologen	4.5	N/A	[55]
T. elongatus	PSI/carboxylated pyrene derivative multi-walled carbon nanotubes	Sodium ascorbate; Methyl viologen	No cyt c: 0.8 Cyt c present: 18	N/A	[34]
R. sphaeroides	PSI-based biohybrid cells	N/A	405630	N/A	[56]
R. sphaeroides	PSI/graphene	Aminomethylferrocene; Coenzyme Q_0	1.2, 0.4	N/A	[57]

‡PSI-based biohybrid solar cells component information with its respective generated photocurrent. PSI source came from the cyanobacteria *Thermosynechococcus elongatus* (orange) and *Rhodobacter sphaeroides* (blue). The HT3 cells are from genetically PSII-modified *Synechocystis* sp. PCC 6803 strain. Electron donors and acceptors are indicated under the redox mediators' category. The photocurrents are reported in uA cm^{-2}. Any unavailable, multiple, or estimated data is indicated with (N/A).

[a] Reference was conducted to improve the photocurrent performance of PSI-based biohybrid cells.

[b] Reference reported other estimated photocurrent values observed in different conditions or solar cell composition.

2.4. *Biofilms, microbial solar cells, and thylakoid membrane-based solar cells*

In this section, we will continue to look at other types of photocurrent producing cells, focusing specifically on biofilms, microbial, and thylakoid membrane-based solar cells. Another type of bioelectrochemical system that generates an observable electric current is microbial fuel cells, which can capture the produced electrons in the chemical reactions. Electrical photocurrents can occur in biofilms through electron transfer across active photosynthetic bacterial membranes [58]. There is a greater prevalence of a redox shuttle mechanism than a direct conduction mechanism in the electron transfer from the bacteria to the electrode. The limitations of this mechanism for devices harvesting solar energy is the charge transferred to the electrode [58].

Bioelectrochemical photocurrent harvesting and photo response rate are enhanced using ternary indium tin oxide (ITO) electrodes with porosities lengths between nanometers and micrometers [58]. Researchers have also demonstrated how to generate the highest electrical power output with a non-sulfur purple bacterium, such as *R. sphaeroides* [56]. A current density of 405.63 mA m^{-2} can be obtained by using *R. sphaeroides* in the anodic part of a microbial fuel cell, permanganate as the cathodic electrolyte, the platinum as the anodic electrode, the graphite as the cathodic electrode, and a 2.1 cm^2 cathodic surface [56].

The difference between biophotovoltaic systems (BPVs) and microbial fuel cells is that the former generates an extracellular electrical current through oxygenic photosynthetic microorganisms upon illumination. BPVs can provide a power density of 0.5 W m^{-2}, which is enough to power small electrical devices. Progress has been made in the development of BPVs in terms of methods to improve efficacy and the utilization of optimal biological materials, electrodes, and interfacial wiring [59].

The intact thylakoid membranes can be used in a photoelectrochemical cell to capture light. The membrane can be adsorbed without a linker by using an aerosol technique and electrohydrodynamic atomization [60]. Under these conditions and upon UV and visible light illumination, the maximum photocurrent density was 6.7 mA cm^{-2}, while a 12 μA cm^{-2} was generated upon visible light illumination [60]. A novel single-junction organic solar cell stack composed of spinach PSI, tyrosine, ITO, C60, and Au would yield a 3470 μA cm^{-2} current density [61].

3. Hydrogen Evolution Photocatalyzed By Biological Reaction Centers

3.1. *Early history of photosynthetic hydrogen production*

It has been known for nearly 80 years that green algae are capable of converting light energy into molecular hydrogen. This observation was initially reported by Hans Gaffron in 1939[62]. Gaffron was later able to demonstrate using inhibitors of the flow of electrons during the light reactions of photosynthesis, that algae were able to catalyze the photoproduction of H_2 via noncyclic electron flow through Photosystem I (PSI) to a hydrogenase enzyme[63]. Further, it was shown[64, 65] that these algae are capable of simultaneously producing oxygen and hydrogen, with a ratio of H_2 to O_2 at 1.9, approaching the theoretical ratio of 2.0[64]. The ability of these algae to produce hydrogen was found to be linked to their ability to express a hydrogenase[66-68] that is capable of accepting electrons donated by PSI. These algal hydrogenases are representative of the class of [FeFe]-type hydrogenases that are linked to the photosynthetic electron transport chain[69]. Although it is accepted that the plastids present in higher plants arose from cyanobacteria, genomic analysis indicates that cyanobacteria contain only [NiFe]-hydrogenases, and appear to lack the [FeFe]-type hydrogenases

that are found in green algae[70, 71]. While these two hydrogenase classes catalyze the same chemical reaction in the end, [NiFe]-types are approximately three times more abundant and tend to be more O_2 tolerant as compared to [FeFe]-type hydrogenases[72]. *In vitro* strategies for hydrogen production utilizing purified biological reaction centers have historically utilized either coupling with a hydrogenase enzyme or platinization of the reaction center, as shown in Figure 4 below.

3.2. ***Bioengineered in vivo hydrogen production***

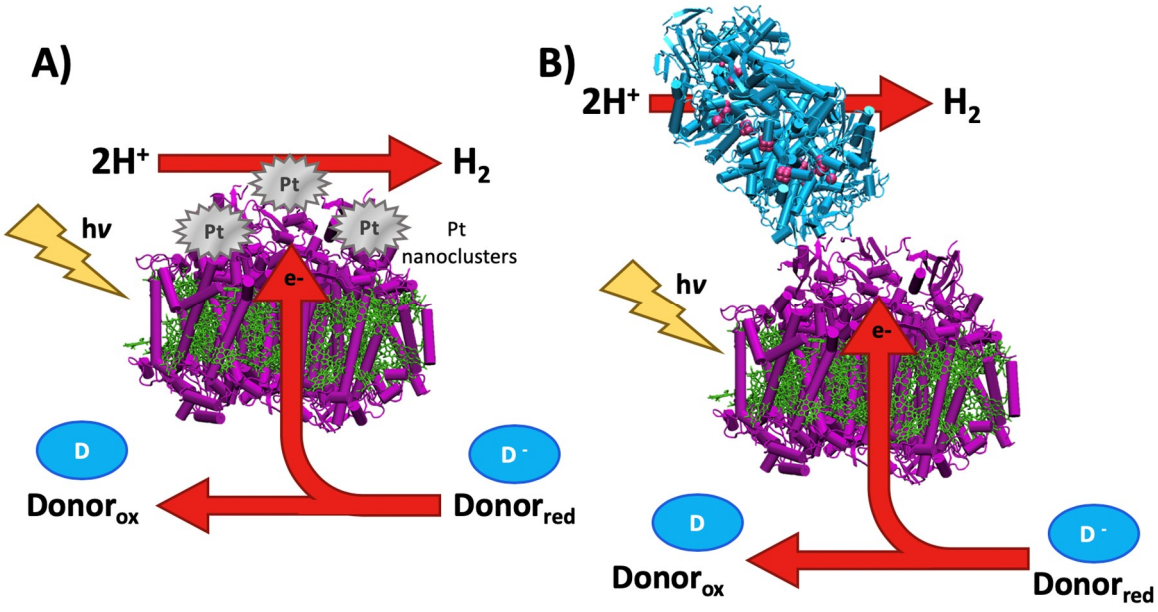

Figure 4. Comparison of methods for hydrogen evolution by reaction centers. Two common methods for reaction center modification for hydrogen evolution are platinization, shown in Figure 4A, and coupling to a hydrogenase enzyme, shown in Figure 4B. Shown in purple in both panels is the protein backbone of PSI, with chlorophyll antenna shown in green. A [Fe-Fe] hydrogenase enzyme is shown in 4B in light blue, with metal clusters shown in pink. The flow of electrons from the donor molecule through the reaction center are shown in red arrows. Figure adapted from [73].

Recently there has been considerable interest in using bio-inspired methods to produce hydrogen as current methods of H_2 fuel production still utilize natural gas, electricity, and conventional CO_2-emitting power plants[74]. In principle, the utilization of either whole photosynthetic organisms or purified biological enzymes is of interest as they can employ the highly efficient process of photosynthesis to produce H_2 from two simple and abundant yet renewable resources, sunlight and water. Previous work has identified two independent pathways of H_2 production catalyzed by photosynthetic organisms that could potentially be utilized for energy production. Greenbaum and co-workers demonstrated the existence of a low-level but continuous electron transport pathway based on oxygenic photosynthesis[75-77]. This is distinct from a second, fermentative, pathway of electron transport for H_2 production reported by Gaffron, Gibbs, and co-workers [63, 66, 78-80]. However, it is now clear that both of these electron-transport processes have limitations in both sustainability and yield. Photosynthetic H_2 production with H_2O as the source of electrons cannot be sustained beyond a few minutes because O_2, derived from the water splitting activity of Photosystem II (PSII), functions to both inactivate the hydrogenase enzyme as well as a negative regulator of hydrogenase expression[71]. On the other hand, hydrogen evolution derived from the catabolism of endogenous substrates in green algae does not have the reservoir capacity to sustain high rates of electron transfer to the photosynthetic apparatus necessary for scaled-up H_2 production.

Although the incompatibility of simultaneous photocatalytic production of O_2 and H_2 remained problematic for many years[81], in the late 1990's a simple and elegant solution was reported[82]. By using a nutrient-induced two-stage growth cycle for photosynthetic organisms the processes of

oxygen evolution and hydrogen production may be separated temporally and is capable of being sustained for hours. Using replete substrate-rich media in stage 1, normal oxygenic photosynthesis occurs, and in stage 2, the algae are deprived of sulfur-containing nutrients. This makes the organisms unable to repair PSII, thus attenuating oxygen evolution as water splitting is not occurring to evolve O_2. This alters the normal pathways of electron transport in photosynthesis; electrons are now derived from substrate donation directly into photosynthetic electron transport without PSII via one or more catabolic processes instead of via water splitting. These electrons are then in turn provided to a hydrogenase via PSI yielding hydrogen. This system has been shown to work in the algae *Chlamydomonas reinhardtii* and has been studied in some detail [83]. *Chlamydomonas reinhardtii* has also shown the ability to utilize chlororespiration catalyzed by PSI and flavodiiron proteins to drastically increase its O_2 uptake rate under high light conditions[84]. This has been found to generate microoxic niches within the thylakoids of *Chlamydomonas*, allowing for microenvironments where its [FeFe] hydrogenases (H_2-ases) are protected from oxidation by molecular O_2, but to also improve hydrogenase catalytic activity even significantly under aerobic culture conditions. Recently, live cyanobacterial cultures have been incorporated into bio-hybrid devices and have been shown to generate a biophotoelectrochemical system capable of producing stable photocurrent and molecular H_2[85].

3.3. *Overcoming kinetic limitations of hydrogen evolution*

As described above, it has been shown that *in vivo* the cyanobacteria and eukaryotic algae and plants utilize the photosynthetic reactions in their thylakoid membranes to divert electrons from PSI under anaerobic conditions towards H_2-producing hydrogenase enzymes (H_2-ases). Unfortunately, it has been shown that in many organisms the [FeFe] H_2-ases are irreversibly inhibited by O_2 which makes this conversion short lived and greatly limits the industrial or economic feasibility of H_2 by these [FeFe] H_2-ases[86]. Moreover, to efficiently couple electron transfer from the water splitting complex in PSII through PSI to the H_2-ase there are three diffusion limited steps: PQ diffusion from PSII; plastocyanin (PC)/cyt c_6 diffusion from the cyt b_6/f complex to PSI; and reduced ferredoxin diffusion from PSI to H_2-ase. All of these processes represent rate limited steps and impose kinetic limits on the overall synthesis.

Early work showed that this diffusion limitation could be overcome in *in vitro* by covalently coupling the electron donor PC to spinach PSI via a chemical crosslinker. Following cross-linking it was observed that the yield of hydrogen production from platinum nanoparticles could be increased >300%[87]. Interestingly, by using bioengineering to directly attach the distal [4Fe-4S] cluster of the [FeFe]H_2-ase from *Clostridium acetobutylicum* to the terminal [4Fe-4S] cluster of F_B on the acceptor side of PSI, a > 2x increased yield in electron flow compared to the *in vivo* oxygenic photosynthesis process was seen. By building this biological/organic biohybrid, the work further demonstrated the feasibility of using synthetic biology methods to tether together and even redesign redox components to overcome diffusion-based rate limitations on electron transfer reactions[88]. More recently, it was observed that some of these diffusion limited reactions could be influenced *in vivo* by genetic manipulation of the grana diameter in the thylakoid membrane ultrastructure[89]. This work clearly demonstrated that plastocyanin diffusion to PSI becomes much slower if the grana diameter exceeds ~500 nm. This work is consistent with prior Brownian diffusion modeling work that indicates that PC diffusion limits electron transport in linear electron transport (LET) where it was observed, that increasing the grana diameter causes a 14-fold reduction in PC diffusion time between the cyt b_6/*f* complexes and PSI[90]. These two reports would suggest that if bioengineering could engineer and significantly restrict the grana diameter that it may be possible to enhance one of these rate limiting steps to allow fast and efficient LET in higher plants and possible observe enhanced H_2 output from cultivated cyanobacteria or algae in bioreactors.

Coupling of these early results suggest that the direct fusion of hydrogenase mutants with PSI via the stromal subunits could provide a much higher rate of *in vivo* hydrogen production. The feasibility

of these PsaD/E hydrogenase fusions has already been shown in cyanobacteria where an artificial fusion protein composed of the membrane-bound [NiFe] hydrogenase from the *Ralstonia eutropha* H16 fused *in vivo* to the peripheral PSI subunit PsaE of the cyanobacterium *Thermosynechococcus elongatus* to yield hydrogen production *[91]*. Following a similar strategy, it was recently reported that the NiFe-hydrogenase (HoxYH) of the cyanobacterium *Synechocystis* sp. PCC 6803 could be directly fused to the stromal-exposed PsaD subunit in PSI. This would allow electrons that would normally go from [4Fe4S] cluster of FB in PSI directly to a soluble ferredoxin carrier to be directly transferred to the NiFe hydrogenase. This psaD-hoxYH cyanobacterial mutant was shown to still fix carbon and able will grow photoautotrophically while also yielding 500 μM H_2 under anaerobic conditions in the light [92]. With a similar approach in *Chlamydomonas* it was also shown that by making a ferredoxin-HydA fusion gene, the bipartite fusion protein was is able to accept photosynthetic electrons from PSI and use them for efficient hydrogen production[93]. They observed that Fd-HydA construct has a ~4.5-fold greater photosynthetic H_2 yield than the native WT HydA *in vivo*. This work has been extended to bring the hydrogenase even closer to PSI by insertion of the HydA sequence into the PsaC subunit. This synthetic construct promoted the self-assembly of the PSI and hydrogenase portions to yield an active in vivo ensemble. Interestingly the algal cells expressing this PSI-hydrogenase chimera continued to make H_2 in a light-dependent fashion for several days [94].

3.4. *In vitro strategies for hydrogen evolution*

However, as mentioned, this extracted PSI must then be either functionalized or linked to a H_2-producing catalyst, either synthetic or biological[95]. An alternative approach to *in vivo* photosynthetic hydrogen production that has been proposed employs biochemically-isolated PSI reaction centers. The same kinetic and structural properties, which are unsurpassed by synthetic systems for electronic current production, similarly make PSI an ideal candidate for inclusion in bio-hybrid H_2 producing devices. In PSI, photon absorption initiates a unidirectional electron transfer sequence that generates a reducing electron over a distance of 6 nm [96], a reaction that is completed within 150 ns [97]. This photocatalysis is highly efficient, with a quantum yield close to 100% [98, 99]. By coupling the low-potential electron-emergent end of PSI complexes (-0.6 V versus SHE) to either platinum nanoparticles [87, 100] or covalently linked hydrogenase [91, 101], the photochemically produced electrons can catalyze the reduction of protons to hydrogen *in vitro.*

The most commonly studied type of functionalization is the platinization of PSI with Pt nanoparticles, first published in 1985 by Greenbaum[102], and has been found to be remarkably stable with over 85 days of photocatalysis reported[73]. In these cases, the Pt was directly deposited onto the surfaces of the photosynthetic catalysts, but other more recent studies found improvements in H_2 production when Pt nanoparticles were tethered using a molecular wire, giving spatial separation between PSI electron generation and Pt-catalyzed H_2 production[103]. This has been further corroborated by molecular dynamics studies on PSI/[FeFe]-hydrogenase enzyme hybrid systems that studied the effect of molecular wire length between the two enzymes on the stability of the system. This system has the potential of utilizing solar energy twice: 1) First, light will be used to grow the photosynthetic organism that will express and assemble the very complex biomolecular hydrogen evolving machinery. 2) Once extracted and functionalized, solar energy will be used to drive photosynthetic electron transport in PSI a second time to produce hydrogen *in vitro*.

There are many potential methods being studied for the improvement of these bio-hybrid H_2-producing systems. As these systems tend to be sensitive to oxygen, there is interest in developing either anaerobic cells or in potentially the incorporation of oxygen and superoxide scrubbers to help improve H_2 yields. One study utilizing platinized PSI and an osmium-based conductive polymer semiconductor for wiring the PSI protein to the electrode found good production of photocurrent through the device, though actual H_2 production was not quantified[104]. Further, while the quantum efficiency of PSI's photoinduced electron generation approaches 100%, a report by Applegate found

a quantum yield of 10-15% when photoexcitation energy between 400-700 nm was assessed[105]. In attempts to improve this quantum yield, Nagakawa *et al.* utilized the addition of an artificial light harvesting dye, Lumogen Red, to improve the wavelengths of light available for PSI photocatalytic activity and saw large improvements over the non-dye modified PSI-Pt constructs[12]. Utilizing a different strategy to improve H_2 yields by reducing the light harvesting chlorophyll pigments in *Chlamydomonas reinhardtii* 5-6 fold yielded approximately 2-5 fold increases in H_2 production depending on the exact mutant strain studied[106].

3.4. *Emerging technologies for bioengineering hydrogen evolution*

The fact that PSI has been shown active in both the solid-state[107] and in solution for over 280 days[108] suggests that we may be able to produce a highly stable, cell-free hydrogen-evolving system that may prove to be a feasible, solar-driven energy solution [109]. Furthermore, future improvements may allow direct electron extraction from water using a coupled PSII to PSI system capable of recapitulating the photosynthetic electron transport chain in a new hybrid nanoparticle similar to what has been done in solution [110] suggests that fully synthetic, biohybrid solar-to-fuel ensembles may be possible. The ability to use solar energy to split water with only H_2 and O_2 as the products is an ideal, carbon-neutral energy goal with considerable promise. One challenge to such a device is to somehow protect the hydrogenases that are sensitive to O_2 by some sort of sequestration similar to how a similarly O_2 sensitive enzyme, nitrogenases, are separated from PSII O_2 evolution in heterocysts [111, 112].

It may be possible to use synthetic biology and nanofabrication to create an immobilization platform that sequesters the hydrogen production chemistry (PSI and catalyst) from the water splitting chemistry (PSII). In this way the O_2 sensitive catalyst, such as the H_2-ase or other catalyst, can be separated from oxygen production by a water-splitting system (PSII or synthetic). One such configuration is shown in Figure 5 where the use of a self-assembled 2D array of PSI and PSII can be supported using some synthetic polymer matrix that replaces a lipid bilayer (Fig. 5E). Recently there has been progress in isolating photosynthetic reaction centers [113, 114] and other electron transport complexes [115] without detergents using styrene maleic acid copolymers. These polymers surround not only the membrane protein(s) but also a significant boundary layer that may stabilize the protein in a more native confirmation. As a synthetic polymer, these SMAs are very amenable to chemical functionalization that may permit crosslinking within the lateral bilayer region [116]. Relevant to this goal, these SMALP proteins have been shown to be more stable [117, 118] and in the case of PSI have even been shown to undergo more rapid photochemistry [119]. These layers can be assembled into a multilaminar array with a conductive nanowire connecting PSII to PSI. Although cyt c_6 is not a normal electron acceptor of PSII, there is over 800 mV of driving force that may enable this alternate path of electron transfer *in vitro* (Fig. 5A). Such a connection has been shown using soluble electron transfer proteins such as cyt. c_6 to ferry electrons between PSII and PSI (Fig. 5B). The diffusion time can be reduced by making a nanowire to bridge this distance. As is shown in Fig. 5c, we have already been able to clone and express a multimeric cyt. c_6 polyprotein of 5 head-to-toe subunits that will assemble correctly in *E. coli*. MD simulations suggest that each cyt-cyt linkage can extend the heme-heme spacing by ~3.0 nm. The final device structure may involve multiple layers of a polymer-embedded PSII-PSI complex. This design will successfully enable O_2 evolution from the splitting of H_2O in one chamber and the hydrogen evolving catalyst producing H_2 in a second chamber (Fig. 5E). By physically separating these two chemical conversions, the device will recapitulate the natural design of how cyanobacteria separate these two processes during nitrogen fixation in a heterocyst.

Preprints (www.preprints.org) | NOT PEER-REVIEWED | Posted: 10 August 2020 doi:10.20944/preprints202008.0234.v1

Peer-reviewed version available at Catalysts 2020, 10, 1016; doi:10.3390/catal10091016

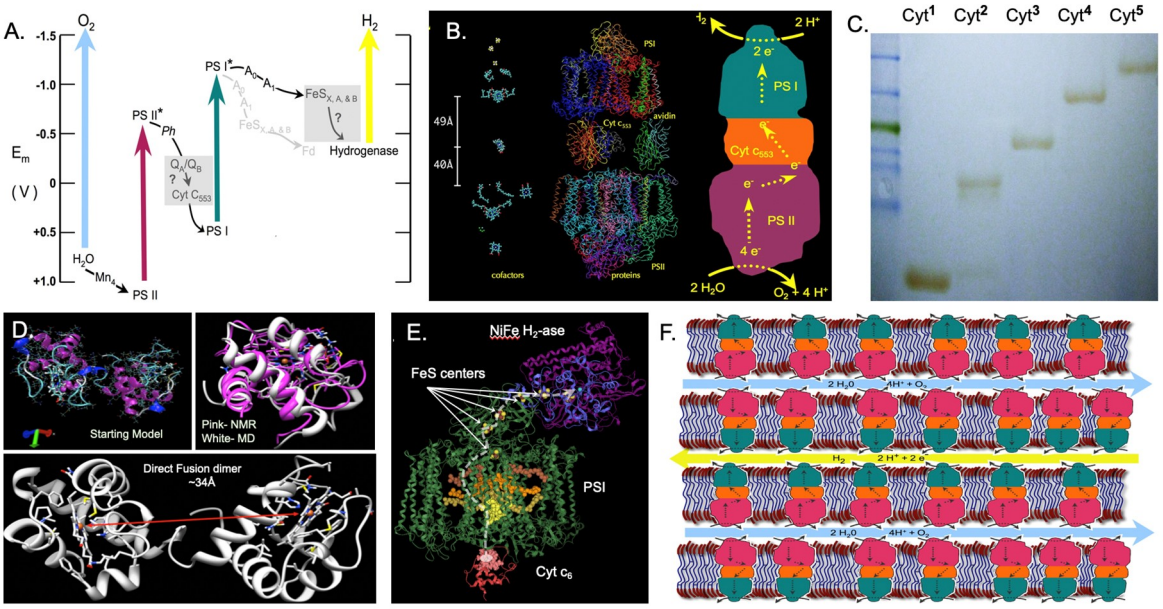

Figure 5. Design of the **OPEC** (Optimized Photosynthetic Energy Converter). **A.** Energy level of the two photosystems in the Z-scheme, changes are shown in the two grey boxes: 1) first box shows the result of with the bypassing of the b_6f complex with cyt c_6 acting as the mobile carrier from PSII to PSI; 2) the second box shows the result of using bioengineering to lower the midpoint potential of the terminal FeS acceptors of PSI ($F_{X, A, B}$) to provide an larger driving force for H_2 production via a hydrogenase or catalyst (not shown). **B.** An avidin-mediated coupling of PSII to PSI via multiple biotinylation of newly inserted, site-directed Cys mutants on the stromal side of PSII and the lumenal side of PSI is shown. The left panel shows the distances of the cofactors that would result from this cross-linking strategy (all distances are shown to scale). The middle panel shows the proteins structures (PSII, cyt.c_6, 3x-avidin, and PSI) based on published PDB files 1IZL, 1C6S, 2AVI, 1JB0). **C.** As is clear from the distance in Panel B the distance from QB to P700 is ~90 Å. To facilitate electron transfer over this long distance we have designed and expressed a linker-less Cyt c6 polyprotein. These gene fusions are reflected by * and demonstrate the ability to make a penta-cyt c_6 polyprotein. **D**. Demonstration of a short 90 msec MD simulation of a di-cyt c_6 fusion protein: the upper left panel shows the backbone trace of the starting fusion protein; the top right shows the superimposition of cyt c_6 monomers based on the starting NMR structure in pink and after the MD simulation; finally the lower panel shows the Fe-Fe distance (~20 Å) of the two hemes following this 90 msec simulation. This would suggest that at least a tetra-cyt c_6 polyprotein would be needed to bridge the PSII-PSI distance shown in B. **E.** Illustration of the direct attachment of a NiFe hydrogenase to the stromal subunit PsaD of PSI with a docked cyt c_6 on the lumenal surface. The path of electron transfer is shown by the dashed grey arrow and the multiple FeS centers are shown with white arrows. **F**. This schematic illustrates how these coupled PSII-cyt c_6-PSI complex could be assembled in a biomimetic polymer that provides a diffusion barrier much like a natural lipid bilayer may function. This complex may be embedded in the amphiphilic polymer (shown in purple) that could be alternated during the assembly process, projecting the oxygen evolving sides of PSII into one microfluidic zone, analogous to the thylakoid lumen (blue) and the hydrogen evolving surface of PSI would be projected into a second microfluidic cavity analogous to the stroma (yellow).

This device illustrates only one possible biohybrid device derived from combining advances in synthetic biology with innovations in material science[3]. Moreover, with the ever-expanding genomics and structural biology already known to existing in extremophiles, suggest many new possible chemical conversions that may be stable at very high temperatures, pressure, and pH extremes [120-122].

4. Bio-Hybrid Photosynthesis with Artificial Reaction Centers

Bio-hybrid, or applied photosynthesis entails coupling man-made light harvesting materials with enzymes for carrying out selected light driven catalytic processes [123-125]. The work discussed in this section will specifically focus on applied photosynthetic systems that do not rely on PSI or PSII for capturing and converting light energy to chemical or electric potential energy. A common thread with all the work presented throughout this review, however, is that an enzyme is key to achieving overall photocatalysis. This approach takes advantage of Nature's ability to do more with less, which is to say enzymes combine high chemical selectivity and turnover rates while using abundant elements. This contrasts with the general reliance on scarce or precious elements as with most highly active inorganic catalysts to generate valuable chemical products.

Oxygenic photosynthetic organisms do not directly couple photochemical reactions to terminal catalysis. The processes of light absorption, charge separation, and initial redox catalysis produces O_2, protons, and reducing equivalents from water, but the products formed directly by PSII and PSI are not the terminal reduced products formed by the photosynthetic organism. Instead, Nature relies on use of specific energy carriers, a small set of reactive chemical species that are generated as a direct result of photosynthesis that then serve as substrates coupled to most all the other enzymatic processes in the organism. These reactive intermediates produced during photosynthesis include plastoquinol, NAD(P)H, ATP, and O_2. This presents a straightforward approach to developing bio-hybrid photosynthetic systems by coupling engineered materials for capturing and converting light to redox equivalents used to generate the reactive intermediate that is then consumed by the enzyme along with the other necessary substrates to achieve the desired catalytic product.

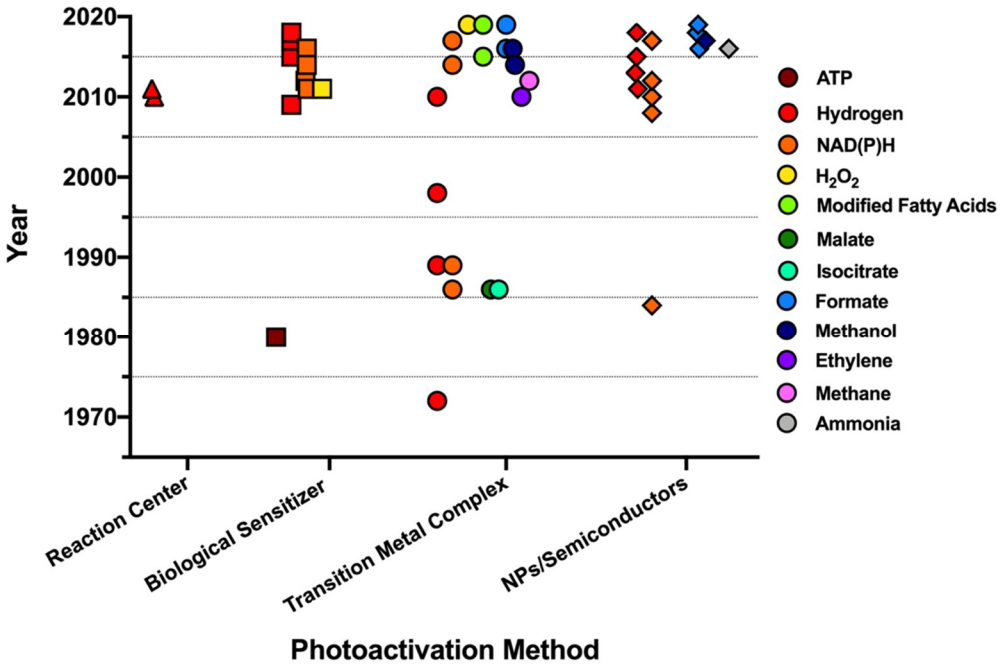

Figure 6. Timeline of selected bio-hybrid artificial photosynthetic studies. This has been organized by light active material and targeted catalytic product. Chemical products are color-coded and separated by photoactivation method.

4.1. *Light Driven ATP Synthesis*

A direct result of the chemical processes of oxygenic photosynthesis is the generation of a proton motive force across the thylakoid membrane. The ATP synthase protein complex couples the dissipation of this proton motive force to the synthesis of adenosine triphosphate (ATP). The work of Moore, Moore, Gust and co-workers used artificial reaction centers [126, 127] based on covalently linked naphthoquinone, porphyrin, and carotenoid moieties imbedded in a liposomal bilayer [128].

Light capture by the artificial reaction center resulted in acidification of the internal volume of the liposome mediated by the lipophilic quinone mediator. An F_0F_1-ATP synthase imbedded in the liposome catalyzed ATP formation by dissipation of the proton gradient across the lipid bilayer resulting in a 7% quantum yield. Other types of reaction centers have been shown to produce membrane potential under visible light irradiation though such activity has not yet been coupled to ATP synthesis [124, 129-131].

4.2. *Bacteriorhodopsin as a catalyst to improve device performances*

Rhodopsins are a family of light-responsive transmembrane proteins found in *Eukaryotes*, *Archaea*, and *Bacteria* [132]. Of particular interest to biotechnological applications is the well-characterized bacteriorhodopsin (bR), first isolated from *Halobacterium salinarum*, which functions as light-driven proton pump [133-135]. Both wild-type and mutant strains of bacteriorhodopsin have been used as light absorbers in dye-sensitized solar cells based on TiO_2 [136-138] and ZnO [139] mesoporous semiconductor surfaces. In such applications, the visible light absorption (λ_{max} = 568 nm) and good photochemical stability of the bound retinal cofactor make bR a good photosensitizer. Recently, the incorporation of bR in a methylammonium lead(II) iodide ($MAPbI_3$) based perovskite solar cell improved the overall energy conversion compared to the same architecture without bR, with performance gain attributed to a decreased charge carrier recombination in the photoactive layer [140]. Such applications do not directly utilize the light induced proton release activity of bR, though some researchers have taken advantage of this to produce photoelectrochemical devices for generating transient photocurrents induced by changes in the local proton concentrations, of interest in the biosensors and wearable devices fields [141, 142].

Both the sensitizer and photon pumping activity of bR has been leveraged in heterogeneous and homogeneous catalytic systems for light driven hydrogen production. Crystalline [143] and amorphous [144] TiO_2 suspensions combined with bR, a sacrificial reductant (e.g., methanol), and Pt catalyst can generate H_2 under illumination with visible light. In a related study, Allam *et al.* observed a more negative onset potential and increased photocurrent densities with bR coated TiO_2 nanotube based photoanodes compared to the same electrodes without bR under photochemical conditions for solar water splitting [145]. Zhao *et al.* found improved electrochemical and photoelectrochemical activity under cathodic bias of carbon-cloth electrodes with surface immobilized coating of bR and Ag nanoparticles (AgNP, ~8 nm diameter) that surpassed that just containing bR or AgNP alone [146].

4.3. *Light-driven enzymatic catalysis by inorganic photocatalysts*

Using a light absorber to convert photon energy to oxidizing or reducing equivalents and then transferring this chemical potential energy to a non-photoactive catalyst to drive a chemical process can overcome the difficult challenge of unifying these two processes in a single chemical species [147]. In early demonstrations of this approach, visible light was used to drive the generation of NADPH and coupled to the chiral specific formation of (–)-2-butanol from 2-butanone using alcohol dehydrogenase [148]. A similar approach using glutamic dehydrogenase formed glutamic acid and the amino acids alanine and aspartic acid [149].

Controlled oxidations can be performed in a similar fashion using alcohol dehydrogenase for substrate specific oxidations. For instance, cyclohexanol can be converted to cyclohexanone or 2-butanol converted to 2-butanone in a photochemical reactor with NADH formed by alcohol dehydrogenase photochemically oxidized to NAD^+ using a (tris-bipyridine) ruthenium(II)) light absorber and MV primary acceptor, with the buildup of reduced MV used to drive the production of H_2 [150]. Flavin-based light absorbers have been used to drive the photochemical formation of H_2O_2 in solution, which in turn serves as co-substrate for the oxyfunctionalization of organic molecules mediated by peroxidase enzymes [151]. Recent work has shown Au-TiO_2 nanoparticles [152] and tandem semiconductor-based PEC systems [153] can be used for the photochemical generation of

H_2O_2 from water to drive such enzymatic processes. The photochemical generation of peroxide was similarly coupled to the formation of olefins from the corresponding fatty acid using the enzyme P450 fatty acid decarboxylase [154]. A variety of other reactions have been carried out via enzyme-assisted photocatalysis such as the selective reduction of acetophenones [155], reduction of carbon–carbon double bonds, [156] [157, 158] and lipase catalyzed alkylation reactions [159] with this work detailed in recent review articles [123, 125].

4.4. *Light-driven enzyme systems for CO_2 reduction*

Artificial photosynthesis endeavors to mimic the overall chemistry of converting water (and CO_2) to oxygen and a fuel (either H_2 or reduced carbon species) with light using technological components [160]. This can entail the exclusive use of inorganic materials [161, 162] or some combination of inorganic, organic, and biological substances combined in some organized way [124, 163-165]. This section will focus on one particular approach to artificial photosynthesis that involves coupling a non-biological light absorber for the light driven production of reducing equivalents to drive an enzymatic process resulting in CO_2 reduction.

Early work by Willner and co-workers demonstrated homogeneous light driven formation of malic acid from pyruvate and CO_2 or isocitric acid from oxoglutaric acid and CO_2 using NADP-malic enzyme and isocitrate dehydrogenase, respectively [166]. The upstream photochemical steps leading to CO_2 fixation involved light absorption by (tris-bipyridine)ruthenium(II) to drive the formation of NADPH in the presence of a sacrificial donor and ferrodoxin-$NADP^+$ reductase. Recent work with nanoparticulate semiconductor photocatalysts have demonstrated similar enzyme mediated C–C bond formation with CO_2 as a substrate [167].

The photochemical reduction of CO_2 to CO was reported by Armstrong and co-workers using TiO_2 nanoparticles with surface adsorbed (tris-bipyridine)ruthenium(II) sensitizer and carbon monoxide dehydrogenase protein [168]. In this approach, the TiO_2 semiconductor nanoparticle mediates electron transfer from the synthetic light absorber to the enzyme to drive catalysis, with a sacrificial donor (EDTA or TEOA) consumed in the regeneration of the ground-state ruthenium chromophore. The system demonstrated a turnover of 0.14 s^{-1} per enzyme over a 4 h period for the production of CO. Reisner and co-workers have used a similar approach for light driven formate production from CO_2 with a turnover frequency of 11 s^{-1} [169].

Another biohybrid approach to CO_2 reduction involves the light driven production of NADH [170] or reduced MV [171] to drive the formation of formic acid by formate dehydrogenase. A variety of light absorbers can be used in these systems including organic dyes such as porphyrins [170, 172], xanthenes [173] , flavins [174] , and perylenes [175] as well as visible light absorbing semiconductors [171, 176-178] , nanostructured materials [179] , polymers [180], and transition metal complexes [181]. If carried out in homogeneous conditions, a sacrificial donor such as EDTA (ethylenediaminetetraacetic acid) or TEOA (triethanolamine) in solution is essential to initiating the photochemical cascade by facilitating the formation of a reducing equivalent from the excited state light absorber. The photogenerated reducing equivalents are used to activate a cocatalyst for driving the production of NADH from NAD^+, with $[(Cp^*)(bpy)Rh(OH_2)]^{2+}$ (Cp^* = pentamethylcyclopentadiene, bpy = 2,2'–bipyridine) a commonly employed catalyst [170, 176, 182]. The formation of formic acid in a complete photochemical reactor has been demonstrated, though this system relied on TEOA for the regeneration of NADH equivalents [170]. A recent study used a hematite photoanode with amorphous cobalt–phosphate water oxidation catalyst to generate reducing equivalents for the enzymatic production of formic acid from CO_2 in the cathodic side of the cell [183]. An applied bias of 0.56 V was required for the onset of photocurrent at pH 7, however, this approach spatially separates the reduced chemical product from the anodic reactions to prevent non-productive re-oxidation to CO_2 which can occur under homogeneous conditions. A similar system with a $BiVO_4$ based photoanode and surface immobilized enzyme coating on the cathode showed spontaneous photocurrent under pH 7 conditions [184]. As the photocurrent, and therefore

rate of production of the reduced product, depends on the photovoltage generated by the PEC under illumination, improved performance has been achieved in enzyme-based PECs by incorporating tandem junctions, such as $BiVO_4$/perovskite systems [185, 186].

The generation of methanol from CO_2 has been pursued using a similar approach as that described above, however, with the additional inclusion of formaldehyde dehydrogenase and alcohol dehydrogenase to the reaction conditions [173]. As each enzyme in the cascade utilizes NADH as a co-substrate, the sequential reduction of CO_2 can proceed with a pool of NADH maintained by the presence of a photocatalyst and Rh-based cocatalyst. Baeg and co-workers demonstrated the production of methanol as the only detected product of CO_2 reduction with a porphyrin based photocatalyst for photo-regeneration of NADH [187]. Park and co-workers employed this same enzyme cascade in a tandem photoelectrochemical cell with a hematite-based photoanode and bismuth ferrite-based photocathode to achieve methanol production from CO_2 with water as the sacrificial source of electrons [188]. While non-spontaneous under illumination, with sufficient applied bias the photochemical tandem cell produced methanol at an average rate of 1280 μmol g_{cat}^{-1} h^{-1}.

4.5. *Light activated nitrogenase*

The reduction of dinitrogen in biology comes concomitant with the hydrolysis of ATP, however, several studies have demonstrated the ability to activate the nitrogenase molybdenum–iron protein photochemically. Using a modified (bis-bipyridine)(phenanthroline)ruthenium(II) complex for covalent attachment to nitrogenase, Tezcan and co-workers first showed the ability drive two electron/two proton reductions, specifically H_2 formation or ethylene formation from acetylene [189]. Subsequent work extended the photochemical activity of the Ru sensitizer conjugated iron–molybdenum protein to the six- electron reduction of hydrogen cyanide to methane [190]. King and co-works later showed the use of CdS nanorods could photosensitize surface adsorbed nitrogenase to drive the formation of ammonia via the eight-electron reduction of N_2 with a turnover frequency of 1.25 s^{-1} [191].

5. Conclusion

Herein, we have reported on recent advances in the generation of photocurrents and the generation of solar fuels in biohybrid solar cells utilizing reaction centers. These include PSI, PSII, and the light harvesting complexes LHCI and LHCII, among others. Several factors must be considered to obtain high photocurrents from biohybrid electrodes and devices. These include electrode material and surface coverage, semiconductor material and architectures, enhancements of reaction center photoexcitation optical cross-sections, electron transfer pathways and redox mediators, as well as electrolytes and working conditions. Optimization of nanostructured biohybrid solar cell devices has increased the generated photocurrent and maximizes the potential of utilizing biological photoactive reaction centers as catalysts for energy and valuable product generation.

Hydrogen has long been considered as an alternative for traditional carbon-based fuels. The biological process of photosynthesis has been able to utilize reaction enter-catalyzed photochemistry to generate molecular hydrogen with great efficiency, though yields *in vivo* historically have been low. Emerging approaches and methods to bioengineer greater yields both *in vivo* and *in vitro* have been discussed herein, and significant improvements have been made especially in areas to improve the activity and stability of these photocatalytic biological reaction centers.

The use of native and synthetic reaction centers to generate light-to-electrical energy conversion is a promising technology to help meet growing energy needs in a sustainable, carbon-neutral manner. Taking this technology a step further to produce valuable chemical products by which the converted solar energy may be stored in the form of chemicals bonds is of great interest. These fuels could then be transported and stored for use at times when solar irradiation is not available. This work in the applied photosynthesis field on improving the magnitude of energy production of biologically-based

photoelectrochemical devices and yields of valuable products from light-coupled enzymatic catalysis hopes to result in a more environmentally friendly production of valuable products and fuels, and help mitigate the need for utilizing fossil fuels and other unsustainable resources.

Author Contributions: AHT and BDB conceptualized this review. AHT, ZYI, EO, JJB, BDS, BDB all contributed to draft preparation, figure making, and editing. The photocurrent section was written by AHT, JJB, EO and ZYI, the hydrogen evolution section by AHT and BDB, and the synthetic photosynthesis section by BDS and AHT. All authors read and approved this review.

Funding: A.H.T. and B.D.B are supported by the Gibson Family Foundation, the Tennessee Plant Research Center, a University of Tennessee at Knoxville (UTK)/Oak Ridge National Laboratory (ORNL) Science Alliance Joint Directed Research Development (JDRD) award to B.D.B., a Dr. Donald L. Akers Faculty Enrichment Fellowship to B.D.B., and National Science Foundation support to B.D.B. (DGE-0801470 and EPS-1004083). A.H.T. was supported by an R25 Fellowship from the National Institutes of Health (R25GM086761).

Acknowledgments: The authors would like to acknowledge the contributions of Dr. Khoa Nguyen (UTK) and Dr. Michael Vaughn (SpectroLogix, Inc. Knoxville) for their contributions to Figure 5.

Conflicts of Interest: The authors declare no conflict of interest.

References

1. Kothe, T. et al. (2014) Engineered electron-transfer chain in photosystem 1 based photocathodes outperforms electron-transfer rates in natural photosynthesis. Chemistry 20 (35), 11029-34.

2. Kazemzadeh, S. et al. (2017) Novel Approach of Biophotovoltaic Solid State Solar Cells Based on a Multilayer of PS1 Complexes as an Active Layer. Acs Sustainable Chemistry & Engineering 5 (11), 9836-9840.

3. Teodor, A.H. and Bruce, B.D. (2020) Putting Photosystem I to Work: Truly Green Energy. Trends Biotechnol.

4. Bennett, T. et al. (2016) Elucidating the role of methyl viologen as a scavenger of photoactivated electrons from photosystem I under aerobic and anaerobic conditions. Phys Chem Chem Phys 18 (12), 8512-21.

5. LeBlanc, G. et al. (2014) Photosystem I Protein Films at Electrode Surfaces for Solar Energy Conversion. Langmuir 30 (37), 10990-11001.

6. Baker, D.R. et al. (2014) Photoelectrochemistry of photosystem I bound in nafion. Langmuir 30 (45), 13650-5.

7. Gordiichuk, P.I. et al. (2016) Filling the Green Gap of a Megadalton Photosystem I Complex by Conjugation of Organic Dyes. Bioconjug Chem 27 (1), 36-41.

8. Balaban, T.S. (2005) Tailoring porphyrins and chlorins for self-assembly in biomimetic artificial antenna systems. Acc Chem Res 38 (8), 612-23.

9. Linke-Schaetzel, M. et al. (2004) Self-assembled chromophores for hybrid solar cells. Thin Solid Films 451, 16-21.

10. Gundlach, K. et al. (2009) Filling the "green gap" of the major light-harvesting chlorophyll a/b complex by covalent attachment of Rhodamine Red. Biochimica Et Biophysica Acta-Bioenergetics 1787 (12), 1499-1504.

11. Dutta, P.K. et al. (2014) Reengineering the optical absorption cross-section of photosynthetic reaction centers. J Am Chem Soc 136 (12), 4599-604.

12. Nagakawa, H. et al. (2019) Efficient hydrogen production using photosystem I enhanced by artificial light harvesting dye. Photochem Photobiol Sci 18 (2), 309-313.

13. Carmeli, I. et al. (2010) Broad band enhancement of light absorption in photosystem I by metal nanoparticle antennas. Nano Lett 10 (6), 2069-74.

14. Dervishogullari, D. et al. (2018) Polyviologen as Electron Transport Material in Photosystem I-Based Biophotovoltaic Cells. Langmuir 34 (51), 15658-15664.

15. Mackowski, S. et al. (2008) Metal-enhanced fluorescence of chlorophylls in single light-harvesting complexes. Nano Lett 8 (2), 558-64.

16. Kim, I. et al. (2011) Metal nanoparticle plasmon-enhanced light-harvesting in a photosystem I thin film. Nano Lett 11 (8), 3091-8.

17. Torres, R. et al. (2018) Effects of gold nanoparticles on the photophysical and photosynthetic parameters of leaves and chloroplasts. Photochem Photobiol Sci 17 (4), 505-516.

18. Niroomand, H. et al. (2018) Tuning the photocurrent generations from photosystem I assembled in tailored biotic-abiotic interfaces. Mrs Communications 8 (3), 823-829.

19. Antonacci, A. and Scognamiglio, V. (2019) Photosynthesis-based hybrid nanostructures: Electrochemical sensors and photovoltaic cells as case studies. Trac-Trends in Analytical Chemistry 115, 100-109.

20. Murray, C.B. et al. (2000) Synthesis and characterization of monodisperse nanocrystals and close-packed nanocrystal assemblies. Annual Review of Materials Science 30, 545-610.

21. Jung, H. et al. (2010) Optical and Electrical Measurement of Energy Transfer between Nanocrystalline Quantum Dots and Photosystem I. Journal of Physical Chemistry B 114 (45), 14544-14549.

22. Nabiev, I. et al. (2010) Fluorescent Quantum Dots as Artificial Antennas for Enhanced Light Harvesting and Energy Transfer to Photosynthetic Reaction Centers. Angewandte Chemie-International Edition 49 (40), 7217-7221.

23. Liu, J.T. et al. (2019) Mechanisms of Self-Assembly and Energy Harvesting in Tuneable Conjugates of Quantum Dots and Engineered Photovoltaic Proteins. Small 15 (4).

24. Yu, D. et al. (2015) Enhanced photocurrent production by bio-dyes of photosynthetic macromolecules on designed TiO2 film. Sci Rep 5, 9375.

25. Hagfeldt, A. et al. (2010) Dye-sensitized solar cells. Chem Rev 110 (11), 6595-663.

26. Kondo, M. et al. (2014) Immobilization of photosystem I or II complexes on electrodes for preparation of photoenergy-conversion devices. Research on Chemical Intermediates 40 (9), 3287-3293.

27. Ciornii, D. et al. (2017) Bioelectronic Circuit on a 3D Electrode Architecture: Enzymatic Catalysis Interconnected with Photosystem I. Journal of the American Chemical Society 139 (46), 16478-16481.

28. Riedel, M. et al. (2018) Light as Trigger for Biocatalysis: Photonic Wiring of Flavin Adenine Dinucleotide-Dependent Glucose Dehydrogenase to Quantum Dot-Sensitized Inverse Opal TiO2 Architectures via Redox Polymers. Acs Catalysis 8 (6), 5212-5220.

29. Simmerman, R.F. et al. (2015) Engineering Photosystem I Complexes with Metal Oxide Binding Peptides for Bioelectronic Applications. Bioconjug Chem 26 (10), 2097-105.

30. Ocakoglu, K. et al. (2014) Photosystem I-based Biophotovoltaics on Nanostructured Hematite. Advanced Functional Materials 24 (47), 7467-7477.

31. Gizzie, E.A. et al. (2015) Electrochemical preparation of Photosystem I-polyaniline composite films for biohybrid solar energy conversion. ACS Appl Mater Interfaces 7 (18), 9328-35.

32. Robinson, M.T. et al. (2017) Photocatalytic photosystem I/PEDOT composite films prepared by vapor-phase polymerization. Nanoscale 9 (18), 6158-6166.

33. Feifel, S.C. et al. (2015) High photocurrent generation by photosystem I on artificial interfaces composed of pi-system-modified graphene. Journal of Materials Chemistry A 3 (23), 12188-12196.

34. Ciornii, D. et al. (2017) Construction of photobiocathodes using multi-walled carbon nanotubes and photosystem I. Physica Status Solidi a-Applications and Materials Science 214 (9).

35. Feifel, S.C. et al. (2015) Unidirectional Photocurrent of Photosystem I on pi-System-Modified Graphene Electrodes: Nanobionic Approaches for the Construction of Photobiohybrid Systems. Langmuir 31 (38), 10590-8.

36. Darby, E. et al. (2014) Photoactive films of photosystem I on transparent reduced graphene oxide electrodes. Langmuir 30 (29), 8990-4.

37. LeBlanc, G. et al. (2012) Enhanced photocurrents of photosystem I films on p-doped silicon. Adv Mater 24 (44), 5959-62.

38. Beam, J.C. et al. (2015) Construction of a Semiconductor-Biological Interface for Solar Energy Conversion: p-Doped Silicon/Photosystem I/Zinc Oxide. Langmuir 31 (36), 10002-7.

39. Stieger, K.R. et al. (2014) Advanced unidirectional photocurrent generation via cytochrome c as reaction partner for directed assembly of photosystem I. Physical Chemistry Chemical Physics 16 (29), 15667-15674.

40. Olmos, J.D.J. et al. (2017) Biofunctionalisation of p-doped silicon with cytochrome c(553) minimises charge recombination and enhances photovoltaic performance of the all-solid-state photosystem I-based biophotoelectrode. Rsc Advances 7 (75), 47854-47866.

41. Ciesielski, P.N. et al. (2008) Functionalized nanoporous gold leaf electrode films for the immobilization of photosystem I. ACS Nano 2 (12), 2465-72.

42. Yamanoi, Y. et al. (2012) Enhanced photocurrent production by photosystem I with modi fi ed viologen derivatives. Thin Solid Films 520 (16), 5123-5127.

43. Yang, S.Y. et al. (2016) Effect of Cross-linking on the Performance and Stability of Photocatalytic Photosystem I Films. Electrochimica Acta 222, 926-932.

44. Pang, H. et al. (2018) Interfacing Photosynthetic Membrane Protein with Mesoporous WO3 Photoelectrode for Solar Water Oxidation. Small 14 (19), e1800104.

45. Ooi, E.J. et al. (2018) Cobalt redox mediators for integration in photosystem I biohybrid solar cells. Abstracts of Papers of the American Chemical Society 255.

46. Zhao, F. et al. (2019) Extended Operational Lifetime of a Photosystem-Based Bioelectrode. J Am Chem Soc 141 (13), 5102-5106.

47. Robinson, M.T. et al. (2018) An Electrochemical Reaction-Diffusion Model of the Photocatalytic Effect of Photosystem I Multilayer Films. J Phys Chem B 122 (1), 117-125.

48. Zhao, F. et al. (2017) Interrogation of a PS1-Based Photocathode by Means of Scanning Photoelectrochemical Microscopy. Small 13 (26).

49. LeBlanc, G. et al. (2014) Photosystem I protein films at electrode surfaces for solar energy conversion. Langmuir 30 (37), 10990-1001.

50. Faulkner, C.J. et al. (2008) Rapid assembly of photosystem I monolayers on gold electrodes. Langmuir 24 (16), 8409-12.

51. Ciesielski, P.N. et al. (2010) Photosystem I - based biohybrid photoelectrochemical cells. Bioresour Technol 101 (9), 3047-53.

52. Gizzie, E.A. et al. (2015) Photosystem I-polyaniline/TiO2 solid-state solar cells: simple devices for biohybrid solar energy conversion. Energy & Environmental Science 8 (12), 3572-3576.

53. Shah, V.B. et al. (2015) Linker-Free Deposition and Adhesion of Photosystem I onto Nanostructured TiO2 for Biohybrid Photoelectrochemical Cells. Langmuir 31 (5), 1675-1682.

54. Stieger, K.R. et al. (2016) Biohybrid architectures for efficient light-to-current conversion based on photosystem I within scalable 3D mesoporous electrodes. Journal of Materials Chemistry A 4 (43), 17009-17017.

55. Feifel, S.C. et al. (2015) Unidirectional Photocurrent of Photosystem I on pi-System-Modified Graphene Electrodes: Nanobionic Approaches for the Construction of Photobiohybrid Systems. Langmuir 31 (38), 10590-10598.

56. Cadirci, B.H. (2018) An electricity production study by Rhodobacter sphaeroides. International Journal of Hydrogen Energy 43 (38), 18001-18006.

57. Csiki, R. et al. (2018) Photocurrent generation of biohybrid systems based on bacterial reaction centers and graphene electrodes. Diamond and Related Materials 89, 286-292.

58. Wenzel, T. et al. (2018) Porous translucent electrodes enhance current generation from photosynthetic biofilms. Nat Commun 9 (1), 1299.

59. Wey, L.T. et al. (2019) The Development of Biophotovoltaic Systems for Power Generation and Biological Analysis. ChemElectroChem 6 (21), 5375-5386.

60. Kavadiya, S. et al. (2016) Directed assembly of the thylakoid membrane on nanostructured TiO2 for a photo-electrochemical cell. Nanoscale 8 (4), 1868-72.

61. Zeynali, A. et al. (2017) Organic solar cell based on photosystem I pigment-protein complex, fabrication and optimization. Organic Electronics 51, 341-348.

62. Gaffron, H. (1939) Reduction of carbon dioxide with molecular hydrogen in green algae. Nature 143, 204-205.

63. Stuart, T.S. and Gaffron, H. (1972) Mechanism of Hydrogen Photoproduction by Several Algae .2. Contribution of Photosystem-Ii. Planta 106 (2), 101-&.

64. Greenbaum, E. (1977) Photosynthetic Unit of Hydrogen Evolution. Science 196 (4292), 879-880.

65. Greenbaum, E. (1980) Simultaneous Photoproduction of Hydrogen and Oxygen by Photosynthesis. Biotechnology and Bioengineering 22, 1-13.

66. Maione, T.E. and Gibbs, M. (1986) Hydrogenase-Mediated Activities in Isolated Chloroplasts of Chlamydomonas reinhardii. Plant Physiol 80 (2), 360-363.

67. Wunschiers, R. et al. (2001) Molecular evidence for a Fe-hydrogenase in the green alga Scenedesmus obliquus. Curr Microbiol 42 (5), 353-60.

68. Winkler, M. et al. (2002) Isolation and molecular characterization of the [Fe]-hydrogenase from the unicellular green alga Chlorella fusca. Biochim Biophys Acta 1576 (3), 330-4.

69. Florin, L. et al. (2001) A novel type of iron hydrogenase in the green alga Scenedesmus obliquus is linked to the photosynthetic electron transport chain. J Biol Chem 276 (9), 6125-32.

70. Ludwig, M. et al. (2006) Occurrence of hydrogenases in cyanobacteria and anoxygenic photosynthetic bacteria: implications for the phylogenetic origin of cyanobacterial and algal hydrogenases. J Mol Evol 63 (6), 758-68.

71. Ghirardi, M.L. et al. (2007) Hydrogenases and hydrogen photoproduction in oxygenic photosynthetic organisms. Annu Rev Plant Biol 58, 71-91.

72. Peters, J.W. et al. (2015) [FeFe]- and [NiFe]-hydrogenase diversity, mechanism, and maturation. Biochim Biophys Acta 1853 (6), 1350-69.

73. Iwuchukwu, I.J. et al. (2010) Self-organized photosynthetic nanoparticle for cell-free hydrogen production. Nature Nanotechnology 5 (1), 73-79.

74. Khanna, N. and Lindblad, P. (2015) Cyanobacterial hydrogenases and hydrogen metabolism revisited: recent progress and future prospects. Int J Mol Sci 16 (5), 10537-61.

75. Greenbaum, E. (1982) Photosynthetic Hydrogen and Oxygen Production: Kinetic Studies. Science 215 (4530), 291-293.

76. Greenbaum, E. et al. (1983) Hydrogen and Oxygen Photoproduction by Marine-Algae. Photochemistry and Photobiology 37 (6), 649-655.

77. Greenbaum, E. (1988) Energetic Efficiency of Hydrogen Photoevolution by Algal Water Splitting. Biophysical Journal 54 (2), 365-368.

78. Stuart, T.S. and Gaffron, H. (1971) Kinetics of Hydrogen Photoproduction by Adapted Scenedesmus. Planta 100 (3), 228-&.

79. Stuart, T.S. and Gaffron, H. (1971) Kinetics of H2 Photoproduction by Scenedesmus. Plant Physiology 47, 32-&.

80. Stuart, T.S. and Gaffron, H. (1972) Mechanism of Hydrogen Photoproduction by Several Algae .1. Effect of Inhibitors of Photophosphorylation. Planta 106 (2), 91-&.

81. Benemann, J.R. et al. (1973) Hydrogen Evolution by a Chloroplast-Ferredoxin-Hydrogenase System. Proc Natl Acad Sci U S A 70 (8), 2317-2320.

82. Melis, A. et al. (2000) Sustained photobiological hydrogen gas production upon reversible inactivation of oxygen evolution in the green alga Chlamydomonas reinhardtii. Plant Physiol 122 (1), 127-36.

83. Melis, A. (2007) Photosynthetic H2 metabolism in Chlamydomonas reinhardtii (unicellular green algae). Planta 226 (5), 1075-86.

84. Liran, O. et al. (2016) Microoxic Niches within the Thylakoid Stroma of Air-Grown Chlamydomonas reinhardtii Protect [FeFe]-Hydrogenase and Support Hydrogen Production under Fully Aerobic Environment. Plant Physiol 172 (1), 264-71.

85. Saper, G. et al. (2018) Live cyanobacteria produce photocurrent and hydrogen using both the respiratory and photosynthetic systems. Nat Commun 9 (1), 2168.

86. Fang, X. et al. (2020) Semi-biological approaches to solar-to-chemical conversion. Chem Soc Rev 49 (14), 4926-4952.

87. Evans, B.R. et al. (2004) Enhanced Photocatalytic Hydrogen Evolution by Covalent Attachment of Plastocyanin to Photosystem I. Nano Letters 4 (10), 1815-1819.

88. Lubner, C.E. et al. (2011) Solar hydrogen-producing bionanodevice outperforms natural photosynthesis. Proceedings of the National Academy of Sciences of the United States of America 108 (52), 20988-20991.

89. Hohner, R. et al. (2020) Plastocyanin is the long-range electron carrier between photosystem II and photosystem I in plants. Proc Natl Acad Sci U S A 117 (26), 15354-15362.

90. Kovalenko, I.B. et al. (2017) Multiparticle Brownian dynamics simulation of experimental kinetics of cytochrome bf oxidation and photosystem I reduction by plastocyanin. Physiol Plant 161 (1), 88-96.

91. Ihara, M. et al. (2006) Light-driven hydrogen production by a hybrid complex of a [NiFe]-hydrogenase and the cyanobacterial photosystem I. Photochem Photobiol 82 (3), 676-82.

92. Appel, J. et al. (2020) Cyanobacterial in vivo solar hydrogen production using a photosystem I–hydrogenase (PsaD-HoxYH) fusion complex. Nature Energy 5 (6), 458-467.

93. Eilenberg, H. et al. (2016) The dual effect of a ferredoxin-hydrogenase fusion protein in vivo: successful divergence of the photosynthetic electron flux towards hydrogen production and elevated oxygen tolerance. Biotechnol Biofuels 9 (1), 182.

94. Kanygin, A. et al. (2020) Rewiring photosynthesis: a photosystem I-hydrogenase chimera that makes H2in vivo. Energy & Environmental Science.

95. Utschig, L.M. et al. (2015) Light-driven hydrogen production from Photosystem I-catalyst hybrids. Current Opinion in Chemical Biology 25, 1-8.

96. Lee, I. et al. (2000) Measurement of electrostatic potentials above oriented single photosynthetic reaction centers. Journal of Physical Chemistry B 104 (11), 2439-2443.

97. Brettel, K. (1997) Electron transfer and arrangement of the redox cofactors in photosystem I. Biochimica Et Biophysica Acta-Bioenergetics 1318 (3), 322-373.

98. Zankel, K.L. et al. (1968) Fluorescence and Photochemical Quenching in Photosynthetic Reaction Centers. Proceedings of the National Academy of Sciences of the United States of America 61 (4), 1243-&.

99. Hiyama, T. (1985) Quantum Yield and Requirement for the Photooxidation of P-700. Physiologie Vegetale 23 (5), 605-610.

100. Millsaps, J.F. et al. (2001) Nanoscale photosynthesis: photocatalytic production of hydrogen by platinized photosystem I reaction centers. Photochem Photobiol 73 (6), 630-5.

101. Ihara, M. et al. (2006) Photoinduced hydrogen production by direct electron transfer from photosystem I cross-linked with cytochrome c3 to [NiFe]-hydrogenase. Photochem Photobiol 82 (6), 1677-85.

102. Greenbaum, E. (1985) Platinized chloroplasts: a novel photocatalytic material. Science 230 (4732), 1373-5.

103. Grimme, R.A. et al. (2008) Photosystem I/molecular wire/metal nanoparticle bioconjugates for the photocatalytic production of H-2. Journal of the American Chemical Society 130 (20), 6308-+.

104. Zhao, F. et al. (2015) Light Induced H2 Evolution from a Biophotocathode Based on Photosystem 1--Pt Nanoparticles Complexes Integrated in Solvated Redox Polymers Films. J Phys Chem B 119 (43), 13726-31.

105. Applegate, A.M. et al. (2016) Quantum yield measurements of light-induced H2 generation in a photosystem I-[FeFe]-H2ase nanoconstruct. Photosynthesis Research 127 (1), 5-11.

106. Ban, S. et al. (2019) Improving hydrogen production of Chlamydomonas reinhardtii by reducing chlorophyll content via atmospheric and room temperature plasma. Bioresour Technol 275, 425-429.

107. Kiley, P. et al. (2005) Self-assembling peptide detergents stabilize isolated photosystem I on a dry surface for an extended time. PLoS Biol 3 (7), e230.

108. Ciesielski, P.N. et al. (2010) Photosystem I - Based biohybrid photoelectrochemical cells. Bioresource Technology 101 (9), 3047-3053.

109. Prince, R.C. and Kheshgi, H.S. (2005) The photobiological production of hydrogen: Potential efficiency and effectiveness as a renewable fuel. Critical Reviews in Microbiology 31 (1), 19-31.

110. Lam, E. and Malkin, R. (1982) Reconstruction of the chloroplast noncyclic electron transport pathway from water to NADP with three integral protein complexes. Proc Natl Acad Sci U S A 79 (18), 5494-5498.

111. Pernil, R. and Schleiff, E. (2019) Metalloproteins in the Biology of Heterocysts. Life (Basel) 9 (2).

112. Queiroz, M.I. et al. (2020) Morphophysiological, structural, and metabolic aspects of microalgae. In Handbook of Microalgae-Based Processes and Products, pp. 25-48.

113. Swainsbury, D.J. et al. (2014) Bacterial reaction centers purified with styrene maleic acid copolymer retain native membrane functional properties and display enhanced stability. Angew Chem Int Ed Engl 53 (44), 11803-7.

114. Brady, N.G. et al. (2019) Non-detergent isolation of a cyanobacterial photosystem I using styrene maleic acid alternating copolymers. Rsc Advances 9 (54), 31781-31796.

115. Sun, C. et al. (2018) Structure of the alternative complex III in a supercomplex with cytochrome oxidase. Nature 557 (7703), 123-126.

116. Schmidt, V. and Sturgis, J.N. (2018) Modifying styrene-maleic acid co-polymer for studying lipid nanodiscs. Biochim Biophys Acta Biomembr 1860 (3), 777-783.

117. Wheatley, M. et al. (2016) GPCR-styrene maleic acid lipid particles (GPCR-SMALPs): their nature and potential. Biochem Soc Trans 44 (2), 619-23.

118. Gulamhussein, A.A. et al. (2019) Examining the stability of membrane proteins within SMALPs. European Polymer Journal 112, 120-125.

119. Cherepanov, D.A. et al. (2020) PSI-SMALP, a Detergent-free Cyanobacterial Photosystem I, Reveals Faster Femtosecond Photochemistry. Biophys J 118 (2), 337-351.

120. Kruger, A. et al. (2018) Towards a sustainable biobased industry - Highlighting the impact of extremophiles. N Biotechnol 40 (Pt A), 144-153.

121. Spieck, E. et al. (2020) Extremophilic nitrite-oxidizing Chloroflexi from Yellowstone hot springs. ISME J 14 (2), 364-379.

122. Shrestha, N. et al. (2018) Extremophiles for microbial-electrochemistry applications: A critical review. Bioresour Technol 255, 318-330.

123. Macia-Agullo, J.A. et al. (2015) Photobiocatalysis: the power of combining photocatalysis and enzymes. Chemistry 21 (31), 10940-59.

124. Fukuzumi, S. et al. (2017) Artificial Photosynthesis for Production of ATP, NAD(P)H, and Hydrogen Peroxide. ChemPhotoChem 2 (3), 121-135.

125. Lee, S.H. et al. (2018) Photobiocatalysis: Activating Redox Enzymes by Direct or Indirect Transfer of Photoinduced Electrons. Angew Chem Int Ed Engl 57 (27), 7958-7985.

126. Gust, D. et al. (2009) Solar fuels via artificial photosynthesis. Acc Chem Res 42 (12), 1890-8.

127. Sherman, B.D. et al. (2014) Evolution of reaction center mimics to systems capable of generating solar fuel. Photosynth Res 120 (1-2), 59-70.

128. Steinberg-Yfrach, G. et al. (1998) Light-driven production of ATP catalysed by F0F1-ATP synthase in an artificial photosynthetic membrane. Nature 392 (6675), 479-82.

129. Numata, T. et al. (2012) Utilization of photoinduced charge-separated state of donor-acceptor-linked molecules for regulation of cell membrane potential and ion transport. J Am Chem Soc 134 (14), 6092-5.

130. Bhosale, S. et al. (2006) Photoproduction of proton gradients with pi-stacked fluorophore scaffolds in lipid bilayers. Science 313 (5783), 84-6.

131. Hvasanov, D. et al. (2013) Self-assembled light-driven photosynthetic-respiratory electron transport chain hybrid proton pump. Chemical Science 4 (10).

132. Ernst, O.P. et al. (2014) Microbial and animal rhodopsins: structures, functions, and molecular mechanisms. Chem Rev 114 (1), 126-63.

133. Schulten, K. and Tavan, P. (1978) A mechanism for the light-driven proton pump of Halobacterium halobium. Nature 272 (5648), 85-6.

134. Mahyad, B. et al. (2015) Bio-nano hybrid materials based on bacteriorhodopsin: Potential applications and future strategies. Adv Colloid Interface Sci 225, 194-202.

135. Li, Y.T. et al. (2018) A Review on Bacteriorhodopsin-Based Bioelectronic Devices. Sensors (Basel) 18 (5).

136. Thavasi, V. et al. (2009) Study on the feasibility of bacteriorhodopsin as bio-photosensitizer in excitonic solar cell: a first report. J Nanosci Nanotechnol 9 (3), 1679-87.

137. Renugopalakrishnan, V. et al. (2014) Engineering a Robust Photovoltaic Device with Quantum Dots and Bacteriorhodopsin. J Phys Chem C Nanomater Interfaces 118 (30), 16710-16717.

138. Mohammadpour, R. and Janfaza, S. (2015) Efficient Nanostructured Biophotovoltaic Cell Based on Bacteriorhodopsin as Biophotosensitizer. ACS Sustainable Chemistry & Engineering 3 (5), 809-813.

139. Molaeirad, A. and Rezaeian, N. (2015) Oriented assembly of bacteriorhodopsin on ZnO nanostructured electrode for enhanced photocurrent generation. Biotechnol Appl Biochem 62 (4), 489-93.

140. Das, S. et al. (2019) Bacteriorhodopsin Enhances Efficiency of Perovskite Solar Cells. ACS Appl Mater Interfaces 11 (34), 30728-30734.

141. Chu, L.K. et al. (2010) Bacteriorhodopsin-based photo-electrochemical cell. Biosens Bioelectron 26 (2), 620-6.

142. Yen, C.W. et al. (2011) Tailoring plasmonic and electrostatic field effects to maximize solar energy conversion by bacteriorhodopsin, the other natural photosynthetic system. Nano Lett 11 (9), 3821-6.

143. Balasubramanian, S. et al. (2013) High-Performance Bioassisted Nanophotocatalyst for Hydrogen Production. Nano Letters 13 (7), 3365-3371.

144. Johnson, K.E. et al. (2018) Development and Characterization of Titanium Dioxide Gel with Encapsulated Bacteriorhodopsin for Hydrogen Production. Langmuir 34 (25), 7488-7496.

145. Allam, N.K. et al. (2011) Bacteriorhodopsin/TiO2 nanotube arrays hybrid system for enhanced photoelectrochemical water splitting. Energy & Environmental Science 4 (8).

146. Zhao, Z. et al. (2015) Bacteriorhodopsin/Ag nanoparticle-based hybrid nano-bio electrocatalyst for efficient and robust H2 evolution from water. J Am Chem Soc 137 (8), 2840-3.

147. Skubi, K.L. et al. (2016) Dual Catalysis Strategies in Photochemical Synthesis. Chem Rev 116 (17), 10035-74.

148. Mandler, D. and Willner, I. (1984) Solar light induced formation of chiral 2-butanol in an enzyme-catalyzed chemical system. Journal of the American Chemical Society 106 (18), 5352-5353.

149. Mandler, D. and Willner, I. (1986) Photoinduced enzyme-catalysed synthesis of amino acids by visible light. Journal of the Chemical Society. Chemical communications (11), 851.

150. Ruppert, R. and Steckhan, E. (1989) Efficient photoelectrochemical in-situ regeneration of NAD(P)+ coupled to enzymatic oxidation of alcohols. Journal of the Chemical Society, Perkin Transactions 2 (7), 811.

151. Gandomkar, S. et al. (2018) Biocatalytic Oxidative Cascade for the Conversion of Fatty Acids into alpha-Ketoacids via Internal H2 O2 Recycling. Angew Chem Int Ed Engl 57 (2), 427-430.

152. Zhang, W. et al. (2018) Selective aerobic oxidation reactions using a combination of photocatalytic water oxidation and enzymatic oxyfunctionalisations. Nat Catal 1 (1), 55-62.

153. Choi, D.S. et al. (2019) Bias-Free In Situ H2O2 Generation in a Photovoltaic-Photoelectrochemical Tandem Cell for Biocatalytic Oxyfunctionalization. ACS Catalysis 9 (11), 10562-10566.

154. Zachos, I. et al. (2015) Photobiocatalytic decarboxylation for olefin synthesis. Chem Commun (Camb) 51 (10), 1918-21.

155. Choudhury, S. et al. (2012) A photocatalyst/enzyme couple that uses solar energy in the asymmetric reduction of acetophenones. Angew Chem Int Ed Engl 51 (46), 11624-8.

156. Hutton, G.A. et al. (2016) Carbon Dots as Versatile Photosensitizers for Solar-Driven Catalysis with Redox Enzymes. J Am Chem Soc 138 (51), 16722-16730.

157. Mifsud, M. et al. (2014) Photobiocatalytic chemistry of oxidoreductases using water as the electron donor. Nat Commun 5, 3145.

158. Peers, M.K. et al. (2016) Light-driven biocatalytic reduction of alpha,beta-unsaturated compounds by ene reductases employing transition metal complexes as photosensitizers. Catal Sci Technol 6 (1), 169-177.

159. Ding, X. et al. (2019) Concurrent Asymmetric Reactions Combining Photocatalysis and Enzyme Catalysis: Direct Enantioselective Synthesis of 2,2-Disubstituted Indol-3-ones from 2-Arylindoles. Angew Chem Int Ed Engl 58 (1), 118-124.

160. Bard, A.J. and Fox, M.A. (1995) Artificial Photosynthesis: Solar Splitting of Water to Hydrogen and Oxygen. Accounts of Chemical Research 28 (3), 141-145.

161. Fujishima, A. and Honda, K. (1972) Electrochemical Photolysis of Water at a Semiconductor Electrode. Nature (London) 238 (5358), 37-38.

162. Khaselev, O. (1998) A Monolithic Photovoltaic-Photoelectrochemical Device for Hydrogen Production via Water Splitting. Science (American Association for the Advancement of Science) 280 (5362), 425-427.

163. Ashford, D.L. et al. (2015) Molecular Chromophore-Catalyst Assemblies for Solar Fuel Applications. Chem Rev 115 (23), 13006-49.

164. Xu, P. et al. (2017) Water splitting dye-sensitized solar cells. Nano Today 14, 42-58.

165. Hambourger, M. et al. (2009) Biology and technology for photochemical fuel production. Chem Soc Rev 38 (1), 25-35.

166. Willner, I. et al. (1986) Photoinduced carbon dioxide fixation forming malic and isocitric acid. Journal of the Chemical Society. Chemical communications (13), 1022.

167. Hamby, H. et al. (2020) Light-driven carbon-carbon bond formation via CO2 reduction catalyzed by complexes of CdS nanorods and a 2-oxoacid oxidoreductase. Proc Natl Acad Sci U S A 117 (1), 135-140.

168. Woolerton, T.W. et al. (2011) CO2 photoreduction at enzyme-modified metal oxide nanoparticles. Energy & Environmental Science 4 (7).

169. Miller, M. et al. (2019) Interfacing Formate Dehydrogenase with Metal Oxides for the Reversible Electrocatalysis and Solar-Driven Reduction of Carbon Dioxide. Angew Chem Int Ed Engl 58 (14), 4601-4605.

170. Yadav, R.K. et al. (2012) A photocatalyst-enzyme coupled artificial photosynthesis system for solar energy in production of formic acid from CO2. J Am Chem Soc 134 (28), 11455-61.

171. Parkinson, B.A. and Weaver, P.F. (1984) Photoelectrochemical pumping of enzymatic CO2 reduction. Nature (London) 309 (5964), 148-149.

172. Kim, J.H. et al. (2011) Zn-containing porphyrin as a biomimetic light-harvesting molecule for biocatalyzed artificial photosynthesis. Chem Commun (Camb) 47 (37), 10227-9.

173. Ji, X. et al. (2016) Integration of Artificial Photosynthesis System for Enhanced Electronic Energy-Transfer Efficacy: A Case Study for Solar-Energy Driven Bioconversion of Carbon Dioxide to Methanol. Small 12 (34), 4753-62.

174. Hofler, G.T. et al. (2018) A Photoenzymatic NADH Regeneration System. Chembiochem 19 (22), 2344-2347.

175. Yadav, R.K. et al. (2016) A highly efficient covalent organic framework film photocatalyst for selective solar fuel production from CO2. Journal of Materials Chemistry A 4 (24), 9413-9418.

176. Park, C.B. et al. (2008) Solar energy in production of L-glutamate through visible light active photocatalyst--redox enzyme coupled bioreactor. Chem Commun (Camb) (42), 5423-5.

177. Nam, D.H. et al. (2010) CdTe, CdSe, and CdS nanocrystals for highly efficient regeneration of nicotinamide cofactor under visible light. Small 6 (8), 922-6.

178. Dibenedetto, A. et al. (2012) Hybrid technologies for an enhanced carbon recycling based on the enzymatic reduction of CO2 to methanol in water: chemical and photochemical NADH regeneration. ChemSusChem 5 (2), 373-8.

179. Ji, X. et al. (2017) Integration of functionalized two-dimensional TaS2 nanosheets and an electron mediator for more efficient biocatalyzed artificial photosynthesis. Journal of Materials Chemistry A 5 (11), 5511-5522.

180. Son, E.J. et al. (2018) Amorphous Carbon Nitride as a Robust Photocatalyst for Biocatalytic Solar-to-Chemical Conversion. ACS Sustainable Chemistry & Engineering 7 (2), 2545-2552.

181. Ryu, J. et al. (2014) Biocatalytic photosynthesis with water as an electron donor. Chemistry 20 (38), 12020-5.

182. Ganesan, V. et al. (2017) Correlation between the Structure and Catalytic Activity of [Cp*Rh(Substituted Bipyridine)] Complexes for NADH Regeneration. Inorg Chem 56 (3), 1366-1374.

183. Nam, D.H. et al. (2016) Enzymatic photosynthesis of formate from carbon dioxide coupled with highly efficient photoelectrochemical regeneration of nicotinamide cofactors. Green Chemistry 18 (22), 5989-5993.

184. Lee, S.Y. et al. (2016) Light-Driven Highly Selective Conversion of CO2

to Formate by Electrosynthesized Enzyme/Cofactor Thin Film Electrode. Advanced Energy Materials 6 (11).

185. Lee, Y.W. et al. (2018) Unbiased biocatalytic solar-to-chemical conversion by FeOOH/BiVO4/perovskite tandem structure. Nat Commun 9 (1), 4208.

186. Kuk, S.K. et al. (2019) Continuous 3D Titanium Nitride Nanoshell Structure for Solar-Driven Unbiased Biocatalytic CO

2

Reduction. Advanced Energy Materials 9 (25).

187. Yadav, R.K. et al. (2014) Highly selective solar-driven methanol from CO2 by a photocatalyst/biocatalyst integrated system. J Am Chem Soc 136 (48), 16728-31.

188. Kuk, S.K. et al. (2017) Photoelectrochemical Reduction of Carbon Dioxide to Methanol through a Highly Efficient Enzyme Cascade. Angew Chem Int Ed Engl 56 (14), 3827-3832.

189. Roth, L.E. et al. (2010) ATP- and iron-protein-independent activation of nitrogenase catalysis by light. J Am Chem Soc 132 (39), 13672-4.

190. Roth, L.E. and Tezcan, F.A. (2012) ATP-uncoupled, six-electron photoreduction of hydrogen cyanide to methane by the molybdenum-iron protein. J Am Chem Soc 134 (20), 8416-9.

191. Brown, K.A. et al. (2016) Light-driven dinitrogen reduction catalyzed by a CdS:nitrogenase MoFe protein biohybrid. Science 352 (6284), 448-50.